

Discovery of Novel Non-Peptidic PAR2 Ligands

Ilona Klösel,¹ Maximilian F. Schmidt,¹ Jonas Kaindl,¹ Harald Hübner,¹ Dorothee Weikert,¹

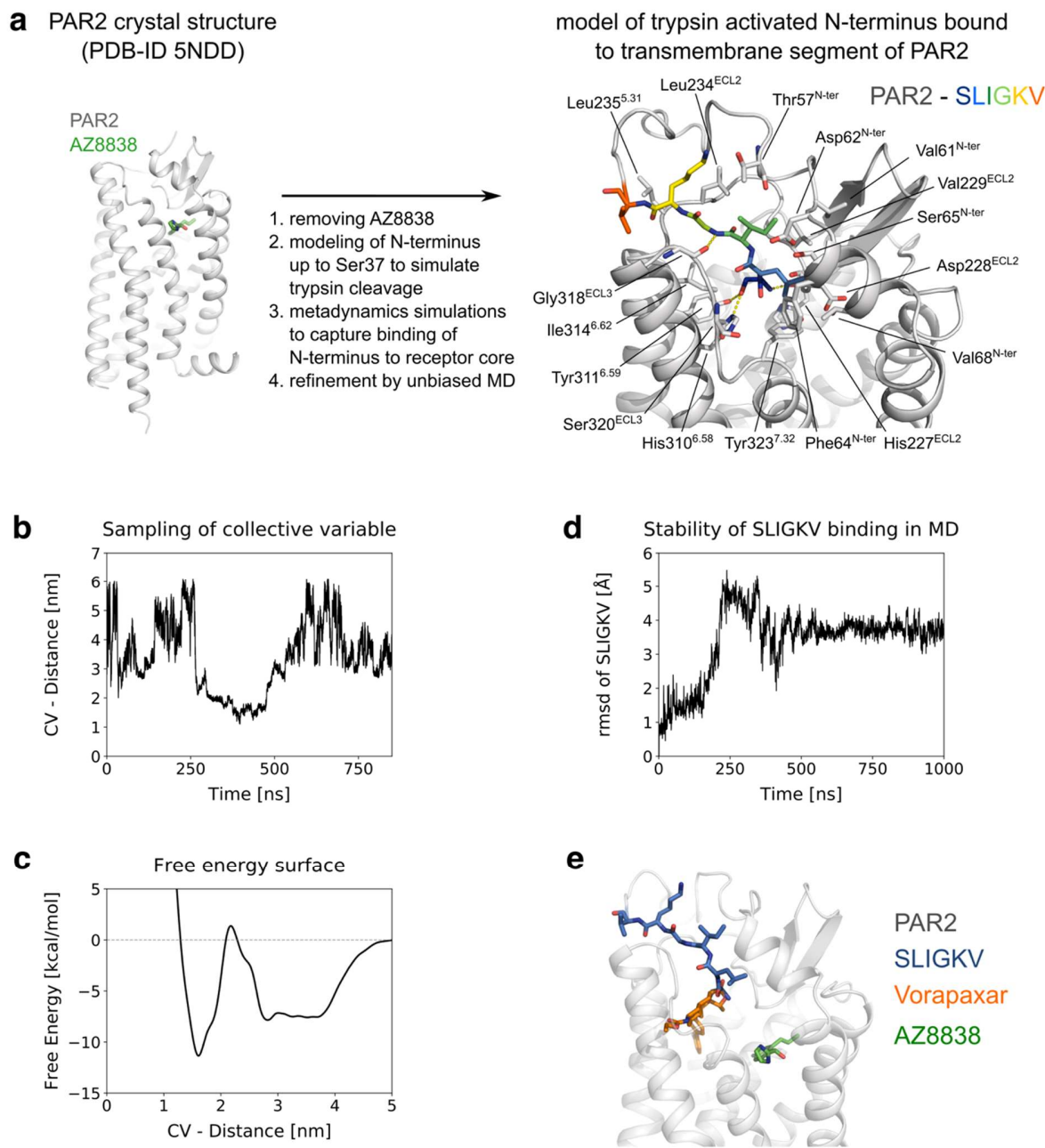
Peter Gmeiner^{1}*

¹Department of Chemistry and Pharmacy, Medicinal Chemistry, Friedrich-Alexander University Erlangen-Nürnberg (FAU), Nikolaus-Fiebiger-Str. 10, 91058 Erlangen, Germany

SUPPORTING INFORMATION

Supplementary Figure S1. Modeling and refinement of trypsin activated PAR2 model.....	2
Supplementary Figure S2. Docking of 4b and 5a to PAR2.....	4
Supplementary Figure S3. Investigation of potential antagonist properties.....	5
Supplementary Table 1. PAINS screening of target and reference compounds.....	6
Supplementary Methods.	8
Supplementary Data. Supplementary Data. ¹ H and ¹³ C NMR spectra of the key compounds.....	28
Supplementary Data. HPLC traces of the key compounds.....	41
Supplementary References.	48

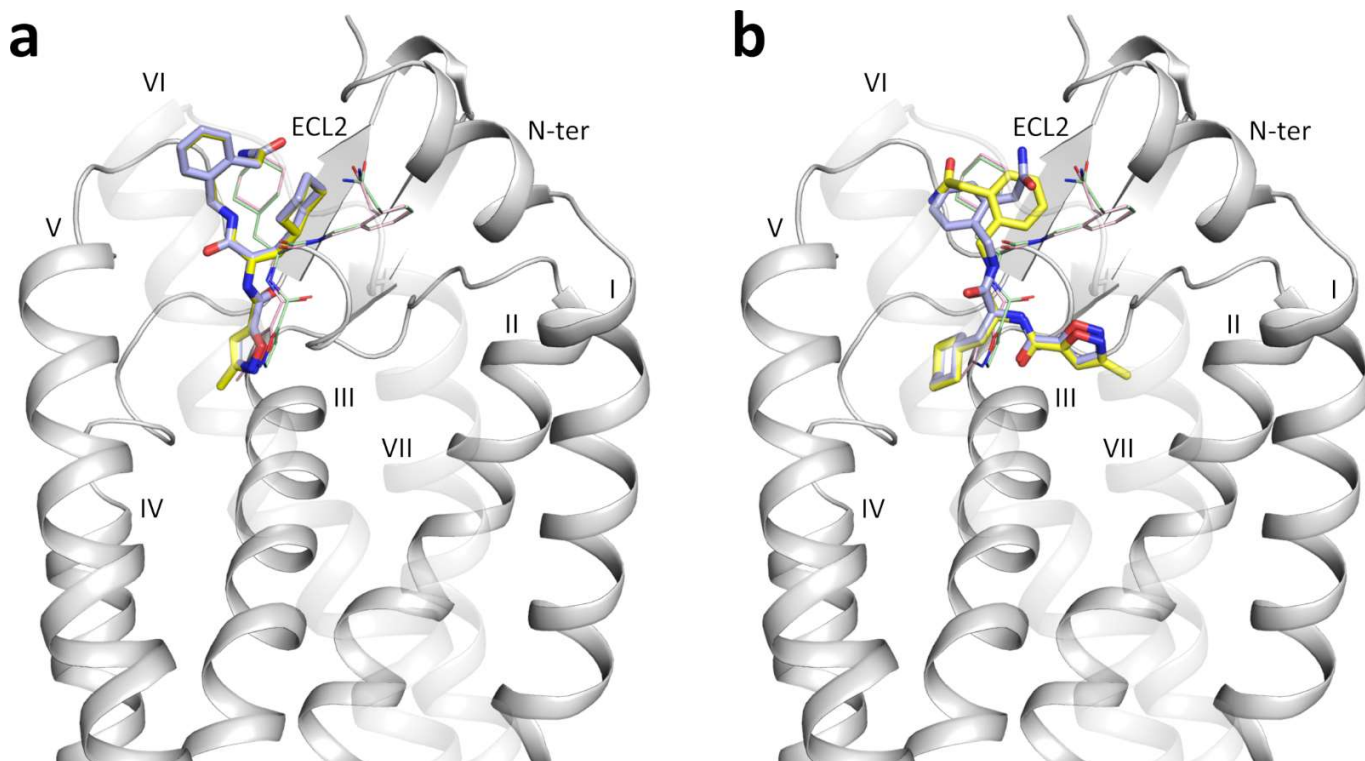
Supplementary Figure S1. Modeling and refinement of trypsin activated PAR2 model.



(a) Applied workflow producing the model of trypsin-activated N-terminus bound to the transmembrane segment of PAR2. Starting from the crystal structure of PAR2 in complex with AZ8838, the coordinates of AZ8838 were removed and N-terminal residues added up to Ser37, to simulate activation by trypsin. After equilibration by unbiased MD, metadynamics simulations were used to sample binding of the tethered ligand to the transmembrane helix bundle. The lowest energy conformation shows the N-terminus bound to the extracellular part of the helix bundle. This conformation was further refined by 1 μ s of unbiased MD. (b) The trace plot depicts the sampling of the collective variable during the metadynamics docking simulations. Panel (c) shows the free-energy surface reconstructed from the metadynamics simulations. This has to be considered a rough estimate of the energy profile and needs to be refined to draw further conclusions. (d) The trace plot

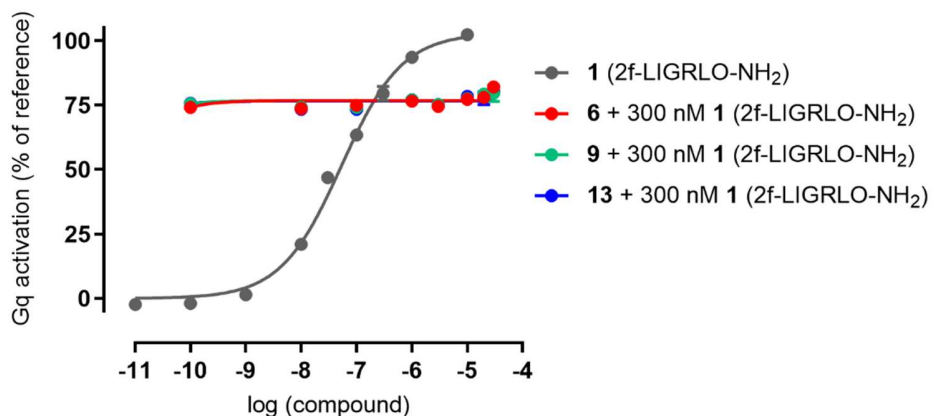
depicts the rmsd of the heavy atoms of the tethered ligand (SLIGKV) to the starting conformation during unbiased MD performed to refine the model of PAR2. After an initial equilibration of about 500 ns, the tethered ligand maintains 1 conformation with constant interactions to the receptor (e) Comparison of ligand binding locations of the tethered ligand in our model, Vorapaxar in the PAR1 crystal structure (PDB-ID 3VW7),¹ and AZ8838 in the PAR2 crystal structure (PDB-ID 5NDD).² The binding site of the tethered ligand in our model partially overlaps with the pocket occupied by the competitive antagonist Vorapaxar in the PAR1. Although Vorapaxar is selective for the PAR1, the location of the location of the binding pocket can be considered to be comparable over the PAR subtypes, as it is for other families of class A GPCRs. The tethered ligand does not overall with the binding site of AZ8838. This agrees with the fact that AZ8838 is considered an allosteric antagonist,² presumably not addressing the orthosteric pocket.

Supplementary Figure S2. Docking of **4b and **5a** to PAR2.**



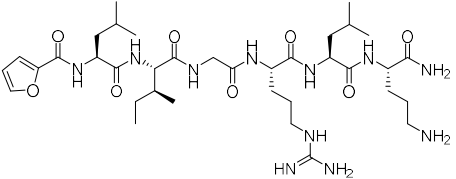
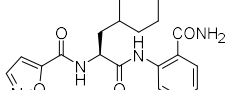
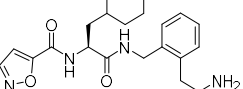
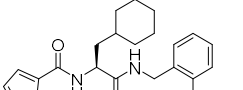
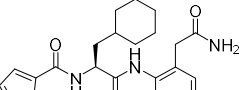
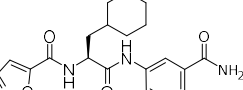
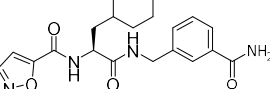
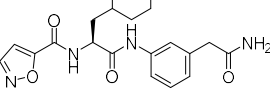
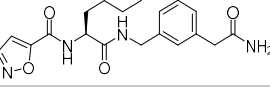
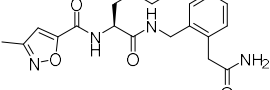
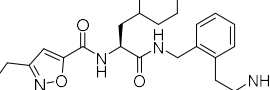
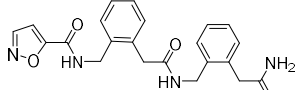
Molecular Docking results for **4b** (blue sticks) and **5a** (yellow sticks) at the PAR2 model of Kennedy et al. (grey)³. Two different clusters (a) and (b) of ligand orientations were observed. For both compounds one representative docking pose is shown. The respective docking poses of **4b** (green lines) and **5a** (pink lines) in the metadynamic model are shown in comparison.

Supplementary Figure S3. Investigation of potential antagonist properties for ligands **6, **9** and **13**.**



Ligands **6**, **9** and **13** were investigated for antagonist properties at PAR2 in the IP₁ accumulation assays. None of the ligands was able to inhibit the effect of the reference agonist **1** (2f-LIGRLO-NH₂) used at a concentration of 300 nM. Data show mean \pm SEM of eight independent experiments, each performed in duplicate.

Supplementary Table 1. PAINS screening of target and reference compounds.^a

Compound	Structure	PAINS/Aggregation liability detected ^b
1		no problems found
4a		no problems found
4b		no problems found
4c		no problems found
4d		no problems found
4e		no problems found
4f		no problems found
4g		no problems found
4h		no problems found
5a		no problems found
5b		no problems found
6		no problems found

^a PAINS screening was performed using the ZINC15 database as described in the methods section. ^b Classification according to ZINC15.

^a PAINS screening was performed using the ZINC15 database as described in the methods section. ^b Classification according to ZINC15.

Supplementary Methods.

General chemistry methods. Reagents and solvents were purchased in their purest grade from abcr, Acros, Alfa Aesar, Sigma Aldrich and TCI and used as without further purification. Compounds were characterized by NMR spectroscopy, IR spectroscopy, high-resolution mass spectra (HRMS) and purity was assessed by rpHPLC. All assayed compounds were $\geq 95\%$ pure. HPLC-MS was run on a BRUKER amaZon SL mass spectrometer using ESI as ionization source. HRMS-ESI was performed on a Bruker Daltonic microTOF II focus TOF-MS spectrometer using ESI or MALDI as ionization source or on a AB Sciex Triple TOF660 SCIex using ESI as ionization source. NMR spectra were obtained on a Bruker Avance 360, Bruker Avance 400 or a Bruker Avance 600 spectrometer at 300 K. ^1H and ^{13}C chemical shifts are given in ppm (δ) relative to TMS in the solvents indicated. In case rotamers were observed, integrals are given as sum over both rotamer signals if not indicated otherwise. IR spectra were performed on a Jasco FT/IR 4100 spectrometer using a film of substance on a NaCl plate. Purification by column chromatography was conducted using silica gel 60 (40-63 μm mesh, Merck) and eluents as binary mixtures with the volume ratios and modifiers indicated. Preparative HPLC was performed on an Agilent 1100 preparative series HPLC system or on an Agilent HPLC 1260 Infinity system combined with a VWD detector. As HPLC column, a ZORBAX-ECLIPSE XDB-C8 PrepHT (21.2 x 150 mm, 5 μm , flow rate 10 - 12 mL/min, $\lambda = 254$ nm) or a ZORBAX-ECLIPSE XDB-C8 PrepHT (30 x 150 mm, 5 μm , usual flow 12 mL/min, $\lambda = 254$ nm) with a BDSpher PUR C8-E (30 x 20 mm, 10 μm) pre-column was used. TLC analyses were performed using Merck 60 F₂₅₄ aluminum sheets and analyzed by UV light (254 nm). Analytical HPLC was performed on an AGILENT 1200 series HPLC system employing a DAD detector. As HPLC column, a ZORBAX ECLIPSE XDB-C8 (4.6 x 150 mm, 5 μm) was used. HPLC purity was measured using the following binary solvent systems: 1) 10% methanol in 0.1% aq. formic acid for 3 min, from 10% to 100% methanol in 15 min, 100% methanol for 6 min, from 100% to 10% methanol in 3 min and 10% methanol for 3 min. 2) 10 – 65% acetonitrile in 0.1% trifluoroacetic acid for 24 min, 65% to 95 % acetonitrile in 2 min, 95 % acetonitrile for 2 min, from 95% to 10 % acetonitrile in 2 min, 10 % acetonitrile for 2 min. For all systems, a flow rate of 0.5 mL/min and a detection wavelength of $\lambda = 220$ nm, 254 nm or 280 nm was employed. The purity of all test compounds was determined to be $>95\%$. Chiral

semi-preparative HPLC was conducted on an AGILENT 1100 series preparative HPLC equipped with a VWD and detection at 220 and 254 nm. As chiral column a DAICEL Chiralpak IC semiprep column (5 μ M, 10 x 250 mm) was used at flow rates from 3 – 6 mL/min with the solvent system indicated. Chiral analytical HPLC was run on a AGILENT series 1100 system equipped with a VWD or DAD and detection at 220 and 254 nm. As chiral column a DAICEL Chiralpak IC column (5 μ M, 4.6 x 250 mm) was used at 20 °C and flow rates from 0.7 mL/min with the solvent system as indicated. Optical rotation values were obtained from a Jasco P2000 polarimeter with the solvents indicated. Melting points were determined in open capillaries using a Büchi 510 melting point apparatus or a MEL-TEMP II apparatus (Laboratory Devices, U.S.A.) and are given uncorrected.

Solid Phase Synthesis. Standard Fmoc SPPS procedures were performed on a Rink amide resin (100 – 200 mesh, 0.66 mmol/g) or on a 2-chlorotriyl chloride resin (200 – 400 mesh, 1.52 mmol/g) in analogy to previously described protocols⁴. In brief, the reactions were carried out in silanized glassware loosely sealed with a silicon septum using a microwave-assisted protocol (Discover microwave oven, CEM Corp.). The corresponding starting material was loaded on the unprotected resin applying a 2 – 5-fold excess, PyBOP, HOBr and DIPEA as coupling reagents and 30 cycles of microwave irradiation (50 W; 10 s). DMF was used as a solvent and the reaction mixture was cooled in an ethanol-ice bath intermittently. If not indicated otherwise, the corresponding amino acids were commercially available and used Fmoc-protected. If present, sidechain-amines were Boc- or Pbf-protected, respectively. Fmoc protective groups were cleaved applying a 25% (v/v) solution of piperidine in DMF and 5 cycles of microwave irradiation (100 W; 5 s). Coupling reactions were performed using the coupling reagents indicated and 20 to 30 cycles of microwave irradiation (50 W; 10 s). Amino acids were used in 5-fold excess and routinely activated by (benzotriazol-1-yloxy)-tritypyrrolidinophosphonium hexafluorophosphate (PyBOP, 5 equivalents) and 1-hydroxybenzotriazole (HOBr, 7.5 equivalents) in presence of DIPEA (5 equivalents). For couplings to primary aromatic amines the corresponding carboxylic acids were activated with HATU (5 equivalents) and DIPEA (10 equivalents) and 30 cycles of microwave irradiation were performed. Cleavage was achieved by treating the resin with a 44:1:3:2

mixture of TFA/TIS/phenol *liquefactum*¹/water for 2 h at ambient temperature (Rink amide resin) or with a 1:4 mixture of HFIP and dichloromethane for 16 h at ambient temperature (Chlorotriyl resin). The crude products were purified by preparative reversed phase HPLC to >95% purity, and characterized by high resolution MS and NMR spectroscopy.

2-Furoyl-Leu-Ile-Gly-Arg-Leu-Orn-NH₂ (TFA salt, 1).⁵ **1** was synthesized applying standard SPPS methods on a Rink amide resin in analogy to previously described protocols.⁵ ESI-MS: *m/z* 778.53 [M+H]⁺, *m/z* 389.8 [M+2H]²⁺. HRMS-ESI: calcd. for C₃₆H₆₅N₁₁O₈, *m/z* 389.7504 [(M+2H)/2]²⁺; found: 389.7503. HPLC (system 1): *t_R* = 13.9 min, purity 96%; (system 2): *t_R* = 15.6 min, purity 95%.

N-{(S)-1-[(S)-2-Amino-1-cyclohexyl-2-oxoethyl)amino]-3-cyclohexyl-1-oxopropan-2-yl}isoxazole-5-carboxamide (AY77, 2).⁶ **2** was synthesized applying standard SPPS methods on a Rink amide resin in analogy to previously described protocols⁶ and purified by preparative HPLC. ESI-MS: *m/z* 405.3 [M+H]⁺. HRMS-ESI: calcd. for C₂₁H₃₂N₄O₄Na, *m/z* 427.2316 [M+Na]⁺; found: 427.2306. HPLC (system 1): *t_R* = 19.9 min, purity 95%; (system 2): *t_R* = 22.6 min, purity 96%.

(S)-N-{1-[(2-Carbamoylphenyl)amino]-3-cyclohexyl-1-oxopropan-2-yl}isoxazole-5-carboxamide (4a). In analogy to previously described protocols,⁷ to a solution of 2-amino-benzoic acid (750 mg, 5.50 mmol) in 1,4-dioxane (20.0 mL) was added a 10wt% solution of sodium carbonate (15.7 mL). Chloroformic acid 9H-fluoren-9-ylmethyl ester (1.68 g, 6.50 mmol) was added and the suspension was stirred at ambient temperature for 2 h. The mixture was acidified with 1 M HCl and extracted with ethyl acetate. The combined organic layers were washed with 1 M HCl and brine, dried over Na₂SO₄ and evaporated. 2-({[(9H-Fluoren-9-yl)methoxy]carbonyl}amino)benzoic acid was obtained as beige solid (1.90 g, 96%) and used without further purification. **4a** was synthesized on a Rink amide resin, loading the resin with 2-({[(9H-fluoren-9-yl)methoxy]carbonyl}amino)benzoic acid and applying standard SPPS methods. Purification by preparative RP-HPLC (40 – 95% CH₃CN/ 0.1% aq. trifluoroacetic acid) yielded **4a** as white solid. IR (NaCl): 3280, 2917, 1671, 1526, 1283, cm⁻¹. ¹H NMR (DMSO-*d*₆, 600 MHz, δ): 12.29 (s, 1H), 9.41 (d, *J* = 7.6 Hz, 1H), 8.77 (d,

¹ phenol *liquefactum* = phenol/water 17:3

J = 1.9 Hz, 1H), 8.53 (dd, *J* = 7.8, 1.4 Hz, 1H), 8.24 (s, 1H), 7.81 (dd, *J* = 8.0, 1.4 Hz, 1H), 7.70 (s, 1H), 7.50 (ddd, *J* = 8.0, 7.6, 1.4 Hz, 1H), 7.21 (d, *J* = 1.9 Hz, 1H), 7.13 (ddd, *J* = 7.8, 7.6, 1.3 Hz, 1H), 4.51 (ddd, *J* = 7.6 Hz, 1H), 1.83 – 1.71 (m, 3H), 1.71 – 1.51 (m, 4H), 1.42 – 1.28 (m, 1H), 1.25 – 1.04 (m, 3H), 1.04 – 0.82 (m, 2H). ^{13}C NMR (DMSO-*d*₆, 151 MHz, δ): 170.6, 170.4, 162.2, 156.1, 151.6, 139.4, 132.3, 128.6, 122.6, 119.8, 119.3, 106.4, 52.3, 38.0, 33.7, 33.2, 31.4, 26.0, 25.7, 25.5. ESI-MS: *m/z* 385.2 [M+H]⁺. HRMS-ESI: calcd. for C₂₀H₂₄N₄O₄Na, 407.1690 [M+Na]⁺; found: 407.1693. $[\alpha]^{22}\text{D}$ -15.5 (C 0.43, CH₃OH). HPLC (system 1): *t*_R = 18.9 min, purity 97%; (system 2): *t*_R = 20.2 min, purity 98%.

(S)-*N*-(1-{|2-(2-Amino-2-oxoethyl)benzyl|amino}-3-cyclohexyl-1-oxopropan-2-yl)isoxazole-5-carboxamide (4b). **4b** was synthesized applying standard SPPS methods on Rink amide resin. Purification by preparative RP-HPLC (40 – 65% CH₃CN/ 0.1% aq. trifluoroacetic acid) yielded **4b** as white solid. IR (NaCl): 3382, 3280, 3200, 2915, 2849, 1665, 1634, 1530, 1422, 1254, 1219 cm⁻¹. ^1H NMR (DMSO-*d*₆, 400 MHz, δ): 8.97 (d, *J* = 8.1 Hz, 1H), 8.73 (d, *J* = 1.9 Hz, 1H), 8.56 (t, *J* = 5.7 Hz, 1H), 7.49 (br s, 1H), 7.25 – 7.17 (m, 4H), 7.17 (d, *J* = 1.9 Hz, 1H), 6.95 (br s, 1H), 4.52 (ddd, *J* = 10.0, 8.1, 5.2 Hz, 1H), 4.33 (d, *J* = 5.7 Hz, 2H), 3.47 (s, 2H), 1.76 – 1.50 (m, 7H), 1.37 – 1.22 (m, 1H), 1.22 – 1.01 (m, 3H), 1.01 – 0.78 (m, 2H). ^{13}C NMR (DMSO-*d*₆, 101 MHz, δ): 172.1, 171.2, 162.3, 155.5, 151.5, 137.4, 134.4, 130.0, 127.4, 126.7, 126.4, 106.0, 50.8, 40.1, 39.0, 38.6, 33.6, 33.0, 31.6, 25.9, 25.6, 25.5. ESI-MS: *m/z* 413.3 [M+H]⁺. HRMS-ESI: calcd for C₂₂H₂₉N₄O₄, 413.2183 [M+H]⁺; found: 413.2190. $[\alpha]^{26}\text{D}$ +1.6 (C 0.43, DMSO). HPLC (system 1): *t*_R = 18.8 min, purity 99%; (system 2): *t*_R = 20.3 min, purity 99%.

(S)-*N*-(1-[(2-Carbamoylbenzyl)amino]-3-cyclohexyl-1-oxopropan-2-yl)isoxazole-5-carboxamide (4c). **4c** was synthesized applying standard SPPS methods on Rink amide resin. Purification by preparative RP-HPLC (40 – 65% CH₃CN/ 0.1% aq. trifluoroacetic acid) yielded **4c** as white solid. IR (NaCl): 3298, 3198, 2920, 2851, 1642, 1628, 1541 cm⁻¹. ^1H NMR (DMSO-*d*₆, 400 MHz, δ): 9.03 (d, *J* = 8.1 Hz, 1H), 8.74 (d, *J* = 1.9 Hz, 1H), 8.52 (t, *J* = 6.1 Hz, 1H), 7.89 (s, 1H), 7.45 (s, 1H), 7.43 (dd, *J* = 7.8, 1.5 Hz, 1H), 7.39 (ddd, *J* = 7.6, 7.5, 1.5 Hz, 1H), 7.34 – 7.25 (m, 2H), 7.17 (d, *J* = 1.9 Hz, 1H), 4.53 (ddd, *J* = 9.8, 8.1, 5.3 Hz, 1H), 4.43 (d, *J* = 6.0 Hz, 2H), 1.76 – 1.53 (m, 7H), 1.36 – 1.24 (m, 1H), 1.22 – 1.02 (m, 3H), 1.00 – 0.80 (m, 2H). ^{13}C NMR (DMSO-*d*₆, 101 MHz, δ): 171.5, 170.5, 162.4, 155.6, 151.6, 137.1, 135.4, 129.6, 127.4, 127.3, 126.5,

106.1, 50.9, 40.2, 38.6, 33.7, 33.1, 31.6, 26.0, 25.7, 25.6. ESI-MS: m/z 399.2 [M+H]⁺. HRMS-ESI: calcd. for C₂₁H₂₇N₄O₄, 399.2027 [M+H]⁺; found: 399.2014. $[\alpha]^{23}_{D}$ -17.0 (c 0.28, CH₃OH). HPLC (system 1): t_R = 17.9 min, purity 96%; (system 2): t_R = 19.9 min, purity 96%.

(S)-N-(1-((2-(2-Amino-2-oxoethyl)phenyl)amino)-3-cyclohexyl-1-oxopropan-2-yl)isoxazole-5-carboxamide (4d). **4d** was synthesized applying standard SPPS methods on Rink amide resin. Purification by preparative RP-HPLC (50 – 65% CH₃CN/ 0.1% aq. trifluoroacetic acid) yielded **4d** as white solid. IR (NaCl): 3302, 3198, 2924, 2852, 1659, 1531, 1448, 1288 cm⁻¹. ¹H NMR (DMSO-*d*₆, 600 MHz, δ): 8.86 (d, *J* = 8.3 Hz, 1H), 8.73 (d, *J* = 1.9 Hz, 1H), 7.49 (br s, 1H), 7.19 – 7.12 (m, 3H), 7.16 (d, *J* = 1.9 Hz, 1H), 7.05 (br s, 1H), 6.78 – 6.74 (m, 1H), 4.44 (ddd, *J* = 10.5, 8.3, 4.7 Hz, 1H), 4.16 (br s, 2H), 1.73 (br d, *J* = 12.7 Hz, 1H), 1.70 – 1.53 (m, 6H), 1.36 – 1.26 (m, 1H), 1.22 – 1.05 (m, 3H), 0.97 – 0.90 (m, 1H), 0.87 (dddd, *J* = 12.7, 12.0, 12.0, 4.0 Hz, 1H), CONH-phenyl was not detected. ¹³C NMR (DMSO-*d*₆, 101 MHz, δ): 173.5, 162.5, 155.5, 151.6, 129.4 (2C), 118.8, 115.2 (2C), 106.1, 50.6, 40.2, 38.8, 33.7, 33.2, 31.6, 26.1, 25.8, 25.6, two quarterny carbons could not be detected. ESI-MS: m/z 399.2 [M+H]⁺. HRMS-ESI: calcd. for C₂₁H₂₇N₄O₄, 399.2027 [M+H]⁺; found: 399.2018. $[\alpha]^{23}_{D}$ -9.2 (c 0.73, CH₃OH). HPLC (system 1): t_R = 17.8 min, purity 99%; (system 2): t_R = 17.2 min, purity 97%.

(S)-N-{1-[(3-Carbamoylphenyl)amino]-3-cyclohexyl-1-oxopropan-2-yl}isoxazole-5-carboxamide (4e). In analogy to previously described protocols,⁷ to a solution of 3-amino-benzoic acid (850 mg, 6.20 mmol) in 1,4-dioxane (20.0 mL) was added a 10wt% solution of sodium carbonate (17.8 mL). Chloroformic acid 9H-fluoren-9-ylmethyl ester (1.91 g, 7.40 mmol) was added and the suspension was stirred at ambient temperature for 3 h. The mixture was acidified with 1 M HCl and extracted with ethyl acetate. The combined organic layers were washed with 1 M HCl and brine, dried over Na₂SO₄ and evaporated. 3-((9H-Fluoren-9-yl)methoxy]carbonyl}amino)benzoic acid was obtained as beige solid (2.11 g, 95%) and used without further purification. **4e** was synthesized on a Rink amide resin, loading the resin with 3-((9H-Fluoren-9-yl)methoxy]carbonyl}amino)benzoic acid and applying standard SPPS methods. Purification by preparative RP-HPLC (40 – 95% CH₃CN/ 0.1% aq. trifluoroacetic acid) yielded **4e** as white solid. IR (NaCl): 3293, 2924, 1662, 1546, 1205, cm⁻¹. ¹H NMR (DMSO-*d*₆, 600 MHz, δ): 10.26 (s, 1H), 9.12 (d, *J* = 7.9 Hz, 1H), 8.76 (d, *J*

= 1.9 Hz, 1H), 8.05 (dd, J = 1.9, 1.9 Hz, 1H), 7.94 (s, 1H), 7.79 (ddd, J = 8.1, 1.9, 1.3 Hz, 1H), 7.55 (ddd, J = 7.8, 1.9, 1.3 Hz, 1H), 7.38 (dd, J = 8.1, 7.9 Hz, 1H), 7.33 (s, 1H), 7.19 (d, J = 1.9 Hz, 1H), 4.67 (ddd, J = 10.5, 7.9, 4.8 Hz, 1H), 1.84 – 1.55 (m, 7H), 1.44 – 1.33 (m, 1H), 1.26 – 1.05 (m, 3H), 1.02 – 0.88 (m, 2H). ^{13}C NMR (DMSO-*d*₆, 151 MHz, δ): 170.7, 167.8, 162.3, 155.7, 151.7, 138.8, 135.1, 128.5, 122.2, 122.1, 119.1, 106.2, 51.7, 38.5, 33.7, 26.0, 25.8, 33.1, 31.6, 25.5. ESI-MS: *m/z* 385.2 [M+H]⁺. HRMS-ESI: calcd. for C₂₀H₂₄N₄O₄Na, 407.1690 [M+Na]⁺; found: 407.1683. HPLC (system 1): *t_R* = 18.5 min, purity 98%; (system 2): *t_R* = 20.1 min, purity 98%.

(S)-*N*-(1-[(3-Carbamoylbenzyl)amino]-3-cyclohexyl-1-oxopropan-2-yl)isoxazole-5-carboxamide (4f). **4f** was synthesized on a Rink amide resin applying standard SPPS methods. Purification by preparative RP-HPLC (40 – 75% CH₃CN/ 0.1% aq. trifluoroacetic acid) yielded **4f** white solid. IR (NaCl): 3408, 2951, 2842, 1656, 1649, 1402, 1020 cm⁻¹. ^1H NMR (DMSO-*d*₆, 400 MHz, δ): 9.03 (d, J = 8.0 Hz, 1H), 8.74 (d, J = 1.9 Hz, 1H), 8.65 (t, J = 5.9 Hz, 1H), 7.91 (br s, 1H), 7.77 (s, 1H), 7.78 – 7.69 (m, 1H), 7.41 – 7.37 (m, 2H), 7.37 (br s, 1H), 7.17 (d, J = 1.9 Hz, 1H), 4.52 (ddd, J = 10.1, 8.0, 5.1 Hz, 1H), 4.32 (d, J = 5.9 Hz, 2H), 1.79 – 1.51 (m, 7H), 1.39 – 1.25 (m, 1H), 1.22 – 1.03 (m, 3H), 1.02 – 0.79 (m, 2H). ^{13}C NMR (DMSO-*d*₆, 101 MHz, δ): 171.5, 167.8, 162.4, 155.7, 151.6, 139.5, 134.3, 129.9, 128.1, 126.4, 125.8, 106.2, 51.0, 42.0, 38.6, 33.7, 33.1, 31.7, 26.1, 25.7, 25.6. ESI-MS: *m/z* 399.3 [M+H]⁺. HRMS-ESI: calcd. for C₂₁H₂₇N₄O₄, 399.2027 [M+H]⁺; found: 399.2026. $[\alpha]^{23}\text{D}$ +11.9 (c 0.97, CH₃OH). HPLC (system 1): *t_R* = 18.5 min, purity 99%; (system 2): *t_R* = 19.5 min, purity 99%.

(S)-*N*-(1-{{3-(2-Amino-2-oxoethyl)phenyl]amino}-3-cyclohexyl-1-oxopropan-2-yl)isoxazole-5-carboxamide (4g). To a solution of 2-(3-aminophenyl)acetic acid (600 mg, 3.97 mmol) in 1,4-dioxane (20.0 mL) a 10wt% solution of sodium carbonate (11.3 mL) was added. Chloroformic acid 9*H*-fluoren-9-ylmethyl ester (1.23 g, 4.75 mmol) was added and the suspension was stirred at ambient temperature for 4 h. The mixture was acidified with 1 M HCl and extracted with ethyl acetate. The combined organic layers were washed with 1 M HCl and brine, dried over Na₂SO₄ and evaporated. Purification by flash chromatography (ethyl acetate/hexane 1:6 + 0.1% glacial acetic acid to 100% ethyl acetate + 0.1% glacial acetic acid) yielded 2-[3-({[(9*H*-fluoren-9-yl)methoxy]carbonyl}amino)phenyl]acetic acid as greyish solid (1.03 g, 69%), which

was loaded in a Rink amide resin. **4g** was synthesized on a Rink amide resin applying standard SPPS methods. Purification by preparative RP-HPLC (40 – 65% CH₃CN/ 0.1% aq. trifluoroacetic acid) yielded **4g** as white solid. IR (NaCl): 3279, 2924, 2852, 1660, 1614, 1555, 1492, 1447, 1300, 1205 cm⁻¹. ¹H NMR (DMSO-*d*₆, 400 MHz, δ): 10.11 (s, 1H), 9.08 (d, *J* = 7.9 Hz, 1H), 8.75 (d, *J* = 1.9 Hz, 1H), 7.52 (ddd, *J* = 7.9, 2.1, 1.8 Hz, 1H), 7.49 (dd, *J* = 1.9, 1.9 Hz, 1H), 7.45 (br s, 1H), 7.22 (dd, *J* = 7.9, 7.8 Hz, 1H), 7.19 (d, *J* = 1.9 Hz, 1H), 6.95 (ddd, *J* = 7.6, 2.1, 1.8 Hz, 1H), 6.87 (br s, 1H), 4.66 (ddd, *J* = 10.4, 7.9, 4.8 Hz), 3.34 (s, 2H), 1.80 – 1.69 (m, 3H), 1.69 – 1.57 (m, 4H), 1.43 – 1.34 (m, 1H), 1.25 – 1.08 (m, 3H), 1.01 – 0.88 (m, 2H). ¹³C NMR (DMSO-*d*₆, 151 MHz, δ): 171.9, 170.4, 162.2, 155.6, 151.5, 138.6, 136.9, 128.3, 124.2, 120.0, 117.4, 106.0, 51.6, 42.1, 38.5, 33.6, 33.0, 31.6, 25.9, 25.7, 25.5. ESI-MS: *m/z* 399.3 [M+H]⁺. HRMS-ESI: calcd. for C₂₁H₂₆N₄O₄Na, 421.1852 [M+Na]⁺; found: 421.1842. $[\alpha]^{23}_D$ +2.2 (c 0.95, CH₃OH). HPLC (system 1): *t*_R = 18.2 min, purity 100%; (system 2): *t*_R = 20.2 min, purity 100%.

(S)-N-(1-{[3-(2-Amino-2-oxoethyl)benzyl]amino}-3-cyclohexyl-1-oxopropan-2-yl)isoxazole-5-carboxamide (4h). **4h** was synthesized on a Rink amide resin applying standard SPPS methods. Purification by preparative RP-HPLC (40 – 65% CH₃CN/ 0.1% aq. trifluoroacetic acid) yielded **4h** as white solid. IR (NaCl): 3312, 3275, 2916, 2850, 1666, 1630, 1543, 1525, 1215 cm⁻¹. ¹H NMR (DMSO-*d*₆, 400 MHz, δ): 8.97 (d, *J* = 8.1 Hz, 1H), 8.74 (d, *J* = 1.9 Hz, 1H), 8.59 (t, *J* = 6.0 Hz, 1H), 7.42 (br s, 1H), 7.23 (dd, *J* = 7.8, 7.7 Hz, 1H), 7.17 (d, *J* = 1.9 Hz, 1H), 7.14 – 7.11 (m, 2H), 7.09 (ddd, *J* = 7.7, 1.5, 1.5 Hz, 1H), 6.85 (br s, 1H), 4.53 (ddd, *J* = 10.1, 8.1, 5.1 Hz, 1H), 4.26 (d, *J* = 6.0 Hz, 2H), 3.34 (s, 2H), 1.75 – 1.55 (m, 7H), 1.37 – 1.26 (m, 1H), 1.24 – 1.04 (m, 3H), 0.99 – 0.81 (m, 2H). ¹³C NMR (DMSO-*d*₆, 151 MHz, δ): 172.0, 171.4, 162.4, 155.6, 151.6, 139.2, 136.4, 129.3, 128.1, 127.5, 125.0, 106.1, 50.9, 42.2, 42.1, 38.7, 33.7, 33.1, 31.6, 26.0, 25.7, 25.6. ESI-MS: *m/z* 413.3 [M+H]⁺. HRMS-ESI: calcd. for C₂₂H₂₉N₄O₄, 413.2183 [M+H]⁺; found: 413.2180. $[\alpha]^{22}_D$ -1.8 (c 0.67, CH₃OH). HPLC (system 1): *t*_R = 18.3 min, purity 97%; (system 2): *t*_R = 19.3 min, purity 97%.

(S)-N-(1-{[2-(2-Amino-2-oxoethyl)benzyl]amino}-3-cyclohexyl-1-oxopropan-2-yl)-3-methylisoxazole-5-carboxamide (5a). **5a** was synthesized applying standard SPPS methods on a Rink amide resin. Purification by preparative RP-HPLC (40 – 65% CH₃CN/ 0.1% aq. trifluoroacetic acid) yielded **5a** as white solid. IR (NaCl): 3309, 3211, 2922, 2850, 1653, 1558, 1541, 1089 cm⁻¹. ¹H NMR (DMSO-*d*₆, 400 MHz,

δ): 8.91 (d, J = 8.1 Hz, 1H), 8.55 (t, J = 5.7 Hz, 1H), 7.51 (s, 1H), 7.25 – 7.16 (m, 4H), 7.01 (s, 1H), 6.96 (s, 1H), 4.50 (ddd, J = 10.1, 8.0, 4.9 Hz, 1H), 4.32 (d, J = 5.7 Hz, 2H), 3.47 (s, 2H), 2.30 (s, 3H), 1.77 – 1.52 (m, 7H), 1.30 – 1.21 (m, 1H), 1.22 – 1.02 (m, 3H), 0.99 – 0.77 (m, 2H). ^{13}C NMR (DMSO-*d*₆, 101 MHz, δ): 172.09, 171.21, 162.62, 160.29, 155.67, 137.38, 134.33, 130.02, 127.38 (2C), 126.64, 126.39, 107.13, 50.71, 39.96, 39.03, 38.71, 33.54, 33.01, 31.49, 25.92, 25.64, 25.47, 10.91. ESI-MS: *m/z* 427.1 [M+H]⁺. HRMS-ESI: calcd. for C₂₃H₃₀NaN₄O₄, 449.2159 [M+Na]⁺; found: 449.2165. $[\alpha]^{23}\text{D}$ -4.323 (c 0.54, CH₃OH). HPLC (system 1): *t*_R = 19.4 min, purity 96%; (system 2): *t*_R = 21.3 min, purity 97%.

(S)-*N*-(1-{|2-(2-Amino-2-oxoethyl)benzyl]amino}-3-cyclohexyl-1-oxopropan-2-yl)-3-ethylisoxazole-5-carboxamide (5b). **5b** was synthesized applying standard SPPS methods on Rink amide resin. Purification by preparative RP-HPLC (40 – 65% CH₃CN/ 0.1% aq. trifluoroacetic acid) yielded **5b** as white solid. IR (NaCl): 3308, 2920, 2850, 1654, 1558, 1541, 1088 cm⁻¹. ^1H NMR (DMSO-*d*₆, 400 MHz, δ): 8.91 (d, J = 8.1 Hz, 1H), 8.56 (t, J = 5.7 Hz, 1H), 7.51 (s, 1H), 7.29 – 7.15 (m, 4H), 7.09 (s, 1H), 6.97 (s, 1H), 4.51 (ddd, J = 10.2, 8.1, 4.9 Hz, 1H), 4.33 (d, J = 5.7 Hz, 2H), 3.47 (s, 2H), 2.70 (q, J = 7.6 Hz, 2H), 1.76 – 1.54 (m, 7H), 1.36 – 1.26 (m, 1H), 1.22 (t, J = 7.6 Hz, 3H), 1.17 – 1.03 (m, 3H), 1.03 – 0.81 (m, 2H). ^{13}C NMR (DMSO-*d*₆, 101 MHz, δ): 172.09, 171.22, 165.47, 162.65, 155.71, 137.39, 134.32, 130.02, 127.36 (2C), 126.64, 126.39, 105.96, 50.72, 39.96, 39.03, 33.52, 33.02, 31.49, 25.93, 25.63, 25.46, 18.80, 12.34. ESI-MS: *m/z* 441.2 [M+H]⁺. HRMS-ESI: calcd. for C₂₄H₃₂NaN₄O₄, 463.2316 [M+Na]⁺; found: 463.2318. $[\alpha]^{23}\text{D}$ -9.2 (c 0.25, CH₃OH). HPLC (system 1): *t*_R = 20.0 min, purity 97%; (system 2): *t*_R = 22.6 min, purity 98%.

N-[2-(2-(2-Amino-2-oxoethyl)benzyl]amino}-2-oxoethyl)benzyl]isoxazole-5-carboxamide (6). **6** was synthesized applying standard SPPS methods on Rink amide resin. Purification by preparative RP-HPLC (40 – 75% CH₃CN/ 0.1% aq. trifluoroacetic acid) yielded **6** as white solid. IR (NaCl): 3302, 2921, 2851, 1658, 1538, 1422 cm⁻¹. ^1H NMR (DMSO-*d*₆, 600 MHz, δ): 9.45 (t, J = 5.8 Hz, 1H), 8.73 (d, J = 1.9 Hz, 1H), 8.63 (t, J = 5.7 Hz, 1H), 7.49 (br s, 1H), 7.31 – 7.17 (m, 8H), 7.08 (d, J = 1.9 Hz, 1H), 6.97 (br s, 1H), 4.55 (d, J = 5.8 Hz, 2H), 4.33 (d, J = 5.6 Hz, 2H), 3.66 (s, 2H), 3.49 (s, 2H). ^{13}C NMR (DMSO-*d*₆, 101 MHz, δ): 172.2, 170.1, 162.5, 155.3, 151.6, 137.3, 136.7, 134.5, 134.5, 130.1, 130.1, 128.2, 127.8, 127.1, 126.8, 126.7, 126.5, 105.7, 40.3, 40.2, 39.8, 39.0. ESI-MS: *m/z* 407.2 [M+H]⁺. HRMS-ESI: calcd. for C₂₂H₂₃N₄O₄, 407.1714

$[M+H]^+$; found: 407.1709. HPLC (system 1): t_R = 16.1 min, purity 100%; (system 2): t_R = 15.7 min, purity 99%.

(S)-N-(1-{[2-(2-Amino-2-oxoethyl)benzyl]amino}-1-oxo-3-phenylpropan-2-yl)isoxazole-5-carboxamide (7). 7 was synthesized applying standard SPPS methods on Rink amide resin. Purification by preparative RP-HPLC (40 – 65% CH_3CN / 0.1% aq. trifluoroacetic acid) yielded 7 as white solid. IR (NaCl): 3314, 3182, 2927, 1646, 1528, 1214 cm^{-1} . ^1H NMR (DMSO- d_6 , 400 MHz, δ): 9.11 (d, J = 8.4 Hz, 1H), 8.70 (d, J = 1.9 Hz, 1H), 8.66 (t, J = 5.7 Hz, 1H), 7.50 (br s, 1H), 7.35 – 7.13 (m, 9H), 7.09 (d, J = 1.9 Hz, 1H), 6.95 (br s, 1H), 4.72 (ddd, J = 10.3, 8.4, 4.5 Hz, 1H), 4.36 (d, J = 5.7 Hz, 2H), 3.47 (s, 2H), 3.16 (dd, J = 13.7, 4.6 Hz, 1H), 3.01 (dd, J = 13.7, 10.4 Hz, 1H). ^{13}C NMR (DMSO- d_6 , 101 MHz, δ): 172.2, 170.3, 162.3, 155.5, 151.6, 137.9, 137.3, 134.5, 130.1, 129.1 (2C), 128.1 (2C), 127.6, 126.8, 126.6, 126.4, 106.0, 54.7, 40.2, 40.2, 37.0. ESI-MS: m/z 407.1 $[M+H]^+$. HRMS-ESI: calcd. for $\text{C}_{22}\text{H}_{23}\text{N}_4\text{O}_4$, 407.1714 $[M+H]^+$; found: 407.1710. $[\alpha]^{22}\text{D}$ -115.6 (c 0.14, CH_3OH). HPLC (system 1): t_R = 17.3 min, purity 95%; (system 2): t_R = 17.7 min, purity 96%.

N-(3-Cyclohexyl-1-((2-methylbenzyl)amino)-1-oxopropan-2-yl)isoxazole-5-carboxamide (8a and 8b). (S)-3-Cyclohexyl-2-(isoxazole-5-carboxamido)propanoic acid was prepared on a 2-chlorotriptyl chloride resin applying standard Fmoc SPPS methods and used without further purification. To a solution of (S)-3-cyclohexyl-2-(isoxazole-5-carboxamido)propanoic acid (88.0 mg, 33.0 μmol), PyBOP (172 mg, 33.0 μmol) and HOBT (66.9 mg, 50.0 μmol) in dichloromethane (4.00 mL) and DMF (0.5 mL) was added DIPEA (60.0 μL , 33.0 μmol) and 2-methylbenzylamine (200 μL , 1.65 mmol). The mixture was irradiated in the microwave reactor (50 W, 10 s) for 30 times, cooling the reaction tube in an ethanol/ice bath between each irradiation step. The solvent was evaporated, and the racemic mixture was purified by preparative HPLC (40 – 65% CH_3CN / 0.1% aq. trifluoroacetic acid). The enantiomers were separated by chiral, semipreparative HPLC (DAICEL Chiralpak IC column, hexane/isopropanol + 0.1% EDA 9:1), referring to the first eluent as **a** and to the second eluent as **b**, to yield **8a** (12.1 mg, 10%) and **8b** (17.0 mg, 14%) as white powder. IR (NaCl): 3285, 3065, 2924, 2852, 1648, 1543, 1449, 1253, 1211, 824, 742 cm^{-1} . ^1H NMR (DMSO- d_6 , 400 MHz, δ): 8.97 (d, J = 8.2 Hz, 1H), 8.74 (d, J = 1.9 Hz, 1H), 8.46 (t, J = 5.7 Hz, 1H), 7.17 (d, J = 1.9 Hz, 1H), 7.24 – 7.10

(m, 4H), 4.55 (ddd, $J = 10.1, 8.1, 5.0$ Hz, 1H), 4.26 (dd, $J = 15.4, 5.7$ Hz, 1H), 4.24 (dd, $J = 15.6, 5.7$ Hz, 1H), 2.25 (s, 3H), 1.76 – 1.54 (m, 7H), 1.38 – 1.24 (m, 1H), 1.23 – 1.04 (m, 3H), 0.99 – 0.80 (m, 2H). ^{13}C NMR (DMSO-*d*₆, 151 MHz, δ): 171.3, 162.4, 155.5, 151.6, 136.8, 135.6, 129.8, 127.5, 126.8, 125.6, 106.0, 50.9, 40.4, 38.8, 33.7, 33.1, 31.7, 26.0, 25.7, 25.6, 18.6. ESI-MS: *m/z* 370.2 [M+H]⁺. HRMS-ESI: calcd. for C₂₁H₂₈N₃O₃, 370.2125 [M+H]⁺; found: 370.2123. $[\alpha]^{27}\text{D}$ (8a, c 0.076, CH₃OH) -6.5; $[\alpha]^{27}\text{D}$ (8b, c 0.13, CH₃OH) +5.5. HPLC (system 1): *t_R* = 20.6 min, purity 100%; (system 2): *t_R* = 27.2 min, purity 100%. Chiral HPLC (hexane/isopropanol + 0.1% EDA 9:1) (8a), *t_R* = 17.5 min, ee 98%; (8b) *t_R* = 20.4, ee 94%.

(S)-*N*-(1-{|2-(2-Amino-2-oxoethyl)benzyl|amino}-3-cyclohexyl-1-oxopropan-2-yl)benzamide (9).

9 was synthesized applying standard SPPS methods on Rink amide resin. Purification by preparative RP-HPLC (40 – 65% CH₃CN/ 0.1% aq. trifluoroacetic acid) yielded **9** as white solid. IR (NaCl): 3389, 3280, 2913, 2850, 1664, 1624, 1392, 1254 cm⁻¹. ^1H NMR (DMSO-*d*₆, 400 MHz, δ): 8.45 (d, $J = 8.0$ Hz, 1H), 8.43 (t, $J = 5.7$ Hz, 1H), 7.94 – 7.88 (m, 2H), 7.58 – 7.41 (m, 4H), 7.27 – 7.14 (m, 4H), 6.95 (br s, 1H), 4.55 (ddd, $J = 10.1, 8.0, 5.1$ Hz, 1H), 4.33 (d, $J = 5.7$ Hz, 2H), 3.48 (s, 2H), 1.78 – 1.53 (m, 7H), 1.40 – 1.29 (m, 1H), 1.26 – 1.02 (m, 3H), 1.00 – 0.81 (m, 2H). ^{13}C NMR (DMSO-*d*₆, 101 MHz, δ): 172.2 (2C), 166.4, 137.7, 134.4, 134.2, 131.2, 130.1, 128.2 (2C), 127.6 (2C), 127.5, 126.7, 126.5, 51.3, 40.0, 39.2, 39.0, 33.8, 33.2, 31.8, 26.1, 25.8, 25.7. ESI-MS: *m/z* 422.2 [M+H]⁺. HRMS-ESI: calcd. for C₂₅H₃₂N₃O₃, 422.2438 [M+H]⁺; found: 422.2436. $[\alpha]^{22}\text{D}$ -29.6 (c 0.44, CH₃OH). HPLC (system 1): *t_R* = 20.0 min, purity 95%; (system 2): *t_R* = 23.2 min, purity 97%.

***N*-(2*S*)-1-{|2-(2-Amino-2-oxoethyl)cyclohexyl|methyl|amino}-3-cyclohexyl-1-oxopropan-2-yl|isoxazole-5-carboxamide (10a and 10b).**

In analogy to previously described protocols,⁸ 2-(2-(aminomethyl)phenyl)acetic acid (1.0 g, 6.1 mmol) and rhodium on alumina (5 wt. %, 30 mg, 0.05 equivalents Rh) were suspended in distilled water (15 ml). The mixture was transferred into a laboratory autoclave and stirred at 100 °C and 18 bar H₂ for 24 h. The crude mixture was filtered through a syringe filter which was washed with distilled water two times. Lyophilization yielded 2-[2-(aminomethyl)cyclohexyl]acetic acid as white solid (0.96 g, 92%), which was used without further purification. To a solution of 2-[2-(aminomethyl)cyclohexyl]acetic acid (250 mg, 1.46 mmol) in 1,4-dioxane (10.0 mL) was added a 10wt% solution of sodium carbonate (4.00 mL). Chloroformic acid 9*H*-fluoren-9-ylmethyl ester (453 mg,

1.75 mmol) was added and the suspension was stirred at ambient temperature for 3 h. The solvent was removed in vacuo and the residue taken up in ethyl acetate (30.0 mL), which was washed with 1 M HCl and brine. The organic layer was dried over Na₂SO₄ and evaporated. Purification by preparative RP-HPLC (40 – 65% CH₃CN/ 0.1% aq. trifluoroacetic acid) yielded 2-{2-[{[(9H-fluoren-9-yl)methoxy]carbonyl}amino)methyl]cyclohexyl}acetic acid as white solid (148 mg, 26%), which was loaded on a Rink amide resin to synthesize compounds **10a** and **10b** applying standard SPPS methods. The corresponding (Z)-diastereomers were separated and purified by preparative RP-HPLC (40 – 65% CH₃CN/ 0.1% aq. trifluoroacetic acid), referring to the first eluent as **a** and to the second one as **b**, to yield **10a** and **10b** as white solids. IR (10a, NaCl): 3208, 3057, 2923, 2849, 1646, 1557, 1442, 1254, 1176 cm⁻¹. ¹H NMR (10a, DMSO-*d*₆, 400 MHz, δ): 8.89 (d, *J* = 8.2 Hz, 1H), 8.73 (d, *J* = 1.9 Hz, 1H), 8.01 (t, *J* = 5.7 Hz, 1H), 7.24 (br s, 1H), 7.16 (d, *J* = 1.9 Hz, 1H), 6.72 (br s, 1H), 4.45 (ddd, *J* = 9.7, 8.1, 5.5 Hz, 1H), 3.06 – 2.89 (m, 2H), 2.13 – 1.96 (m, 3H), 1.79 – 1.03 (m, 19H), 1.01 – 0.78 (m, 3H). ¹³C NMR (10a, DMSO-*d*₆, 151 MHz, δ): 174.0, 171.2, 162.4, 155.4, 151.6, 106.0, 50.9, 40.1, 39.9, 38.9, 33.7, 33.0 (2C), 31.8, 28.7, 26.0 (2C), 25.9, 25.7 (2C), 25.6 (2C). ESI-MS (10a): *m/z* 419.2 [M+H]⁺. HRMS-ESI (10a): calcd. for C₂₂H₃₅N₄O₄, 419.2653 [M+H]⁺; found: 419.2635. $[\alpha]^{24}_D$ +1.5 (10a, c 0.068, CH₃OH). HPLC (10a) (system 1): *t*_R = 19.7 min, purity 96%; (system 2): *t*_R = 21.0 min, purity 97%. IR (10b, NaCl): 3234, 3067, 2922, 2849, 1646, 1572, 1536, 1453, 1260 cm⁻¹. ¹H NMR (10b, DMSO-*d*₆, 400 MHz, δ): 8.90 (d, *J* = 8.1 Hz, 1H), 8.73 (d, *J* = 1.9 Hz, 1H), 8.01 (t, *J* = 5.8 Hz, 1H), 7.23 (br s, 1H), 7.16 (d, *J* = 1.9 Hz, 1H), 6.73 (br s, 1H), 4.45 (ddd, *J* = 9.0, 8.1, 6.1 Hz, 1H), 3.10 (ddd, *J* = 13.3, 8.8, 5.7 Hz, 1H), 2.88 (ddd, *J* = 13.3, 5.7, 5.6 Hz, 1H), 2.09 – 1.96 (m, 3H), 1.77 – 1.04 (m, 20H), 0.99 – 0.80 (m, 2H). ¹³C NMR (10b, DMSO-*d*₆, 151 MHz, δ): 173.9, 171.0, 162.3, 155.4, 151.5, 105.9, 50.9, 40.0, 39.8, 38.8, 33.6, 32.9 (2C), 31.8, 28.5, 25.9 (2C), 25.8, 25.6 (2C), 25.5 (2C). ESI-MS (10b): *m/z* 419.2 [M+H]⁺. HRMS-ESI (10b): calcd. for C₂₂H₃₅N₄O₄, 419.2653 [M+H]⁺; found: 419.2640. $[\alpha]^{24}_D$ -2.9 (10b, c 0.086, CH₃OH). HPLC (10b) (system 1): *t*_R = 20.0 min, purity 98%; (system 2): *t*_R = 21.3 min, purity 98%.

N-[(S)-1-((S)-3-Carbamoyl-3,4-dihydroisoquinolin-2(1H)-yl)-3-cyclohexyl-1-oxopropan-2-yl]isoxazole-5-carboxamide (11). **11** was synthesized applying standard SPPS methods on Rink amide resin. Purification by preparative RP-HPLC (40 – 75% CH₃CN/ 0.1% aq. trifluoroacetic acid) yielded **11** as white

solid. IR (NaCl): 3282, 2923, 2852, 1674, 1645, 1538, 1447, 1436, 1209 cm⁻¹. ¹H NMR (DMSO-*d*₆, 600 MHz, two rotamers were observed, δ): 9.13 and 9.11 (d, *J* = 8.2 Hz, 1H), 8.75 and 8.71 (d, *J* = 1.9 Hz, 1H), 7.36 and 7.31 (br s, 1H), 7.20 – 7.16 (m, 4H), 7.16 and 7.14 (d, *J* = 1.9 Hz, 1H), 6.92 (br s, 1H), 5.11 and 4.94 (ddd, *J* = 9.8, 8.1, 4.5 Hz, 1H), 4.88 and 4.85 (d, *J* = 15.0 Hz, 1H), 4.85 and 4.80 (dd, *J* = 5.9, 2.5 Hz, 1H), 4.64 and 4.36 (d, *J* = 15.2 Hz, 1H), 3.33 and 3.10 (dd, *J* = 13.8, 2.4 Hz, 1H), 3.11 and 3.06 (dd, *J* = 13.9, 5.8 Hz, 1H), 1.91 and 1.84 (br d, *J* = 12.7 Hz, 1H), 1.76 – 1.48 (m, 6H), 1.44 – 1.35 and 1.35 – 1.28 (m, 1H), 1.27 – 1.08 (m, 3H), 1.04 – 0.86 (m, 2H). ¹³C NMR (DMSO-*d*₆, 101 MHz, two rotamers were observed, δ): 172.2, 170.8 and 170.7, 162.0 and 161.9, 155.4 and 155.3, 151.6 and 151.5, 133.4 and 132.3, 133.2 and 132.1, 128.1 and 127.7, 126.8, 126.3 and 126.2, 125.7, 106.2 and 106.0, 54.3 and 52.7, 47.4 and 47.3, 45.0 and 43.1, 38.7 and 37.8, 33.5, 33.3 and 33.2, 31.7 and 31.6, 31.0, 26.0 and 25.9, 25.7 and 25.7, 25.6 and 25.5. ESI-MS: *m/z* 425.2 [M+H]⁺. HRMS-ESI: calcd. for C₂₃H₂₈N₄O₄Na, 447.1997 [M+Na]⁺; found: 447.1991. [α]_D²³ -27.5 (c 0.69, CH₃OH). HPLC (system 1): *t*_R = 19.5 min, purity 100%; (system 2): *t*_R = 22.4 min, purity 99%.

N-[(2*S*)-1-(4-Carbamoyl-3,4-dihydroisoquinolin-2(1*H*)-yl)-3-cyclohexyl-1-oxopropan-2-yl]isoxazole-5-carboxamide (12a and 12b). To a solution of 1,2,3,4-tetrahydroisoquinoline-4-carboxylic acid (250 mg, 1.41 mmol) in 1,4-dioxane (10.0 mL) was added a 10wt% solution of sodium carbonate (4.00 mL). Chloroformic acid 9*H*-fluoren-9-ylmethyl ester (438 mg, 1.69 mmol) was added and the suspension was stirred at ambient temperature for 3 h. The mixture was acidified with 1 M HCl and extracted with ethyl acetate. The combined organic layers were washed with 1 M HCl and brine, dried over Na₂SO₄ and evaporated. (RS)-2-{[(9*H*-Fluoren-9-yl)methoxy]carbonyl}-1,2,3,4-tetrahydroisoquinoline-4-carboxylic acid was obtained as beige solid (650 mg, 98%) and used without further purification. **12a** and **12b** were synthesized on a Rink amide resin, loading the resin with (RS)-2-{[(9*H*-Fluoren-9-yl)methoxy]carbonyl}-1,2,3,4-tetrahydroisoquinoline-4-carboxylic acid and applying standard SPPS methods. Purification was done by preparative RP-HPLC (40 – 65% CH₃CN/ 0.1% aq. trifluoroacetic acid). Diastereomer separation was achieved by RP-HPLC (60 – 68% methanol/ 0.1% aq. trifluoroacetic acid in 10 min; 68 – 100% in 10 min), referring to the first eluent as **a** and to the second one as **b**, to yield **12a** and **12b** as white solids. IR (12a, NaCl): 3298, 2924, 2852, 1671, 1637, 1535, 1448, 1284, 1205, 740 cm⁻¹. ¹H NMR (12a, DMSO-*d*₆, 400 MHz, two rotamers

were observed δ): 9.16 and 9.05 (d, J = 8.1 Hz, 1H), 8.73 (d, J = 1.9 Hz, 1H), 7.68 and 7.56 (s, 1H), 7.27 – 7.19 (m, 5H), 7.18 and 7.14 (d, J = 1.9 Hz, 1H), 5.08 and 5.04 (ddd, J = 11.1, 8.2, 3.7 Hz, 1H), 4.78 and 4.64 (d, J = 17.2 Hz, 1H), 4.72 and 4.56 (d, J = 17.2 Hz, 1H), 4.18 – 4.13 (m, 1H) 4.10 and 3.82 (dd, J = 13.3, 4.6 Hz, 1H), 3.74 and 3.55 (dd, J = 13.3, 4.6 Hz, 1H) 1.89 – 1.47 (m, 7H), 1.45 – 0.74 (m, 6H). ^{13}C NMR (12a, DMSO- d_6 , 151 MHz, two rotamers were observed, δ): 172.9 and 172.8, 170.2 and 169.9, 162.0, 155.3 and 155.2, 151.5, 133.6 and 133.5, 133.1 and 133.0, 128.0 and 127.8, 126.8 and 126.7, 126.5, 126.4 and 126.1, 106.0, 47.1 and 46.6, 44.9 and 44.5, 44.1 and 42.6, 40.0 and 39.9, 38.1 and 37.9, 33.6 and 33.5, 33.2 and 33.0, 31.8 and 31.4, 25.9 and 25.8, 25.7, 25.5 and 25.4. ESI-MS (12a): m/z 425.3 [M+H] $^+$. HRMS-ESI (12a): calcd. for $\text{C}_{23}\text{H}_{28}\text{N}_4\text{O}_4\text{Na}$: 447.1997 [M+Na] $^+$, found: 447.1991. $[\alpha]^{23}\text{D}$ (12a) +26.7 (c 0.67, CH_3OH) HPLC (12a, system 2): t_R = 21.4 min, purity 99%.

IR (12b, NaCl): 3267, 2924, 2853, 1671, 1637, 1535, 1448, 1283, 1205, 741 cm^{-1} . ^1H NMR (12b, DMSO- d_6 , 400 MHz, two rotamers were observed, δ): 9.08 and 8.98 (d, J = 7.9 Hz, 1H), 8.74 and 8.72 (d, J = 1.9 Hz, 1H), 7.64 and 7.60 (s, 1H), 7.28 – 7.20 (m, 4H), 7.18 and 7.13 (d, J = 1.9 Hz, 1H, isoxazole-H4), 7.18 and 7.10 (s, 1H), 5.07 and 4.99 (ddd, J = 11.2, 7.9, 3.7 Hz, 1H), 4.81 and 4.72 (d, J = 16.2 Hz, 1H), 4.71 and 4.50 (d, J = 16.2 Hz, 1H), 3.94 – 3.68 (m, 3H), 1.93 – 1.78 (m, 1H), 1.78 – 1.43 (m, 6H), 1.42 – 1.27 (m, 1H), 1.26 – 1.03 (m, 3H), 1.03 – 0.78 (m, 2H). ^{13}C NMR (12b, DMSO- d_6 , two rotamers were observed, 151 MHz, δ): 172.9 and 172.4, 170.2 and 170.1, 162.1 and 162.0, 155.3 and 155.1, 151.6 and 151.5, 133.7 and 133.3, 133.3 and 132.9, 127.9 and 127.5, 126.8 and 126.7, 126.5, 126.2, 106.0 and 105.9, 47.3 and 47.0, 46.4, 44.1 and 42.3, 39.9 and 39.8, 37.8 and 36.4, 33.6, 33.2 and 33.1, 31.5 and 31.5, 25.9 and 25.9, 25.6 and 25.6, 25.5. ESI-MS (12b): m/z 425.3 [M+H] $^+$. HRMS-ESI (12b): calcd. for $\text{C}_{23}\text{H}_{28}\text{N}_4\text{O}_4\text{Na}$, 447.1997 [M+Na] $^+$; found: 447.1999. $[\alpha]^{23}\text{D}$ (12b) -17.3 (c 0.46, CH_3OH). HPLC (12b, system 2): t_R = 21.2 min, purity 99%.

(S)-N-(1-{|2-(2-Amino-2-oxoethyl)benzyl|amino}-3-cyclohexyl-1-oxopropan-2-yl)-N-methylisoxazole-5-carboxamide (13). In analogy to previously described protocols,⁹ Fmoc-3-cyclohexyl-*L*-alanine (393 mg, 1.00 mmol), paraformaldehyde (200 mg, 6.66 mmol) and *p*-toluenesulfonic acid (20.0 mg, 0.116 mmol) were suspended in toluene (20.0 mL) and heated under reflux in a Dean-Stark set up for 16 h. The cooled mixture was washed with saturated, aqueous sodium bicarbonate solution and the organic layer

was dried over Na_2SO_4 . Evaporation of the solvent yielded (9*H*-fluoren-9-yl)methyl (*S*)-4-(cyclohexylmethyl)-5-oxooxazolidine-3-carboxylate as light yellow oil (403 mg, 99%) which was used without further purification. (9*H*-Fluoren-9-yl)methyl (*S*)-4-(cyclohexylmethyl)-5-oxooxazolidine-3-carboxylate (300 mg, 0.74 mmol) and aluminium chloride (197 mg, 1.48 mmol) were dissolved in anhydrous dichloromethane (15.0 mL). Triethylsilane (0.24 mL, 1.48 mmol) was added and the mixture was stirred at ambient temperature for 16 h. The crude mixture was diluted with dichloromethane (5.00 mL) and washed with 1 M HCl. The organic layer was dried over Na_2SO_4 and evaporated to yield (*S*)-2-({[(9*H*-fluoren-9-yl)methoxy]carbonyl}(methyl)amino)-3-cyclohexylpropanoic acid as beige oil (253 mg, 84%) which was used without any further purification and loaded on a Rink Amide resin to synthesize **13** applying standard SPPS methods. Purification by preparative RP-HPLC (40 – 65% CH_3CN / 0.1% aq. trifluoroacetic acid) yielded **13** as white solid. IR (NaCl): 3318, 3208, 2925, 1667, 1532, 1400, 737 cm^{-1} . ^1H NMR ($\text{DMSO}-d_6$, 400 MHz, two rotamers were observed, δ): 8.75 and 8.73 (d, J = 1.9 Hz, 1H), 8.66 and 8.58 (t, J = 5.7 Hz, 1H), 7.51 (br s, 1H), 7.27 – 7.13 (m, 4H), 7.03 and 6.80 (d, J = 1.9 Hz, 1H), 6.96 (br s, 1H), 5.11 and 4.99 (dd, J = 10.3, 5.4 Hz, 1H), 4.40 and 4.34 (dd, J = 11.4, 5.7 Hz, 2H), 3.49 (s, 2H), 3.03 and 2.92 (s, 3H), 1.85 – 1.50 (m, 7H), 1.37 – 0.69 (m, 6H). ^{13}C NMR ($\text{DMSO}-d_6$, 101 MHz, two rotamers were observed, δ): 172.3, 169.6 and 169.3, 162.4, 159.4 and 158.8, 151.0 and 150.9, 137.5 and 137.4, 134.6 and 134.5, 130.2, 127.8 and 127.6, 126.6 and 126.9, 126.8, 106.9 and 105.9, 58.5 and 54.4, 40.4 and 40.2, 39.2, 36.1 and 35.4, 33.9 and 33.7, 33.2 and 33.0, 32.5 and 29.7, 31.7 and 31.5, 26.0 and 25.9, 25.8, 25.6 and 25.4. ESI-MS: m/z 427.1 [$\text{M}+\text{H}$] $^+$. HRMS-ESI: calcd. for $\text{C}_{23}\text{H}_{31}\text{N}_4\text{O}_4$ 427.2340 [$\text{M}+\text{H}$] $^+$; found: 427.2331. $[\alpha]^{24}_{\text{D}} -45.5$ (c 0.68, CH_3OH). HPLC (system 1): $t_{\text{R}} = 19.5$ min, purity 98%; (system 2): $t_{\text{R}} = 22.1$ min, purity 98%.

***N*-(*(S*)-3-Cyclohexyl-1-{|(*(S*)-1-cyclohexyl-2-(dimethylamino)-2-oxoethyl|amino}-1-oxopropan-2-yl)isoxazole-5-carboxamide** (14). *(S*)-2-Cyclohexyl-2-[(*S*)-3-cyclohexyl-2-(isoxazole-5-carboxamido)propanamido]-acetic acid was synthesized applying standard Fmoc-based SPPS methods on a 2-chlorotriptyl resin and purified by preparative HPLC. A solution of (*S*)-2-cyclohexyl-2-[(*S*)-3-cyclohexyl-2-(isoxazole-5-carboxamido)propanamido]-acetic acid (40 mg, 0.10 mmol) in dichloromethane/DMF (3:1, 2.0 mL) was cooled to 0 °C. TBTU (48 mg, 0.15 mmol) was dissolved in DMF (0.5 mL), DIPEA was added

(30 μ L, 0.15 mmol) and the mixture was added dropwise. The reaction was stirred at 0 °C for 15 minutes before a 2 M solution of dimethylamine in THF (60 μ L, 0.12 mmol) was added. It was stirred for another 30 minutes at ambient temperature. After evaporation of the volatile components the crude product was purified by preparative HPLC (*column 1*; acetonitrile/H₂O + 0.1% TFA, 40% 1 min, gradient 40 – 95% in 11 min, 95% 2 min, gradient 95 – 40% 1 min, 40% 1 min; t_R = 8.3 min) to yield **14** as white solid (17 mg, 39%). IR (NaCl): 3318, 3208, 2925, 1667, 1532, 1400, 737 cm⁻¹. ¹H NMR (DMSO-*d*₆, 400 MHz, δ): 8.92 (d, *J* = 8.3 Hz, 1H), 8.75 (d, *J* = 1.9 Hz, 1H), 8.04 (d, *J* = 8.6 Hz, 1H), 7.15 (d, *J* = 1.9 Hz, 1H), 4.60 – 4.49 (m, 2H), 3.04 (s, 3H), 2.81 (s, 3H), 1.78 – 1.45 (m, 13H), 1.35 – 1.22 (m, 1H), 1.23 – 1.04 (m, 6H), 1.03 – 0.80 (m, 4H). ¹³C NMR (DMSO-*d*₆, 101 MHz, δ): 171.1, 170.8, 162.4, 155.3, 151.7, 106.2, 52.6, 50.8, 38.8, 36.9, 35.1, 33.7, 33.2, 31.7, 29.1, 28.1, 26.1, 25.8, 25.8, 25.7, 25.6, 25.5 (2C). ESI-MS: *m/z* 433.2 [M+H]⁺. HRMS-ESI: calcd. for C₂₃H₃₇N₄O₄: *m/z* 433.2809 [M+H]⁺, found: 433.2806. $[\alpha]^{24}_D$ -14.0 (c 0.47, CH₃OH). HPLC (system 1) t_R = 20.7 min, purity 98%; (system 2) t_R = 25.3 min, purity: 97%.

Cell culture. Cell culture reagents were obtained from gibco or Invitrogen LifeTechnologies GmbH. HEK-293T cells were grown in DMEM/F-12 medium supplemented with 10% fetal bovine serum, 100 μ g/mL penicillin, 100 μ g/mL streptomycin and 0.5 mg/mL *L*-glutamine in culture dishes (\varnothing 10 cm) at 37 °C and 5% CO₂ to a confluence of 70 – 100%. Cells were split every three to four days and used for experiments between passages 3 and 14.

β -Arrestin-HEK-293 cells were grown in DMEM/F-12 medium supplemented with 10% fetal bovine serum, 100 μ g/mL penicillin, 100 μ g/mL streptomycin, 150 μ g/mL hygromycin and 0.5 mg/mL *L*-glutamine in culture dishes (\varnothing 10 cm) at 37 °C and 5% CO₂ to a confluence of 70 – 100%. Cells were split every three to four days and used for experiments between passages 3 and 16. For subcultivation of HEK-293T cells and β -Arrestin-HEK-293 cells, the medium was removed, and cells were detached with 2 mL of Versene. 8 mL of medium was added, and cells were gently pipetted up and down to separate aggregates. After centrifugation (220 x g_E, 6 min), cells were resuspended in 10 mL fresh medium and plated onto new culture dishes in the appropriate density.

Transient transfection. HEK-293T cells or β -arrestin-HEK-293 cells were plated onto culture dishes and grown to a confluence of 50 – 80% at 37 °C and 5% CO₂. 1 h to 3 h prior to transfection the medium was renewed with DMEM/F-12 medium supplemented with 10% fetal bovine serum, 100 μ g/mL penicillin and 100 μ g/mL streptomycin and 0.5 mg/mL L-glutamine. The transfection mix was prepared using 800 μ L serum free medium, 3 μ g cDNA and 9 μ L Mirus TransIT-293 (for \varnothing 10 cm culture dishes), adding the components in the order indicated and only mixing it gently once Mirus TransIT was contained. After pre-incubation for 20 – 30 min at room temperature, the mix was added dropwisely. Medium was renewed 24 h after transfection and cultivation was continued for further 24 h at 5% CO₂, 37 °C, before cells were used for experiments.

IP-One accumulation assay. Measurement of PAR2- respectively G_{aq}-stimulated IP1 formation was performed using the IP-One HTRF® assay (CisBio, Codolet, France) according to the manufacturer's protocol. In brief, HEK-293T cells transiently transfected with human PAR2 applying Mirus TransIT 293 as transfection reagent, were detached from the culture dish with Versene (Life Technologies, Darmstadt, Germany), seeded into black, clear flat bottom 384-well plates (Greiner, Frickenhausen, Germany) in assay medium at a density of 10,000 cells/well and maintained at 37 °C, 5% CO₂ for 24 h. The medium was exchanged with stimulation buffer and cells were incubated with dilutions of the test compounds in stimulation buffer for 2 h at 37 °C, 5% CO₂. For antagonist assays, cells were preincubated with the antagonists for 30 min, before 2f-LIGRLO-NH₂ (final concentration 300 nM) was added and the incubation was continued for 90 min. After incubation, freshly prepared IP1 reagent mix (in lysis buffer), then freshly prepared AB reagent mix (in lysis buffer) was added and cells were further incubated in the dark for 60 min at ambient temperature. FRET ratios (emission at 620-10 nm and 665-10 nm, respectively) were determined using the CLARIOstar II plate reader (BMG LabTech, Ortenberg, Germany). Results were analyzed by non-linear regression using the algorithms of PRISM 6.0 to obtain an EC₅₀ and normalized to basal (0%) and the maximal effect of 2f-LIGRLO-NH₂ (100%) for the calculation of efficacy (E_{max}).

β -Arrestin-2 recruitment assay. Measurement of receptor stimulated β -arrestin-2 recruitment was performed using the PathHunter assay (DiscoverX, Birmingham, U.K.) as described previously.¹⁰ In brief,

(EA)- β -arrestin-2-HEK293 cells were transiently transfected with the ProLink tagged PAR2-PK1s construct, applying Mirus TransIT 293 as transfection reagent. 24 h after transfection, cells were detached from the culture dish using with Versene (Life Technologies, Darmstadt, Germany), seeded into white, clear flat bottom 384-well plates (Greiner, Frickenhausen, Germany) in assay medium at a density of 5,000 cells/well and maintained at 37 °C, 5% CO₂ for 24 h. After incubation with the test compounds dissolved in PBS for 90 min at 37 °C, the detection mix was added, and incubation was continued in the dark for 60 min at room temperature. Chemiluminescence was determined using the CLARIOstar II plate reader (BMG LabTech, Ortenberg, Germany). Results were analyzed by non-linear regression using the algorithms of PRISM 6.0 to obtain an EC₅₀ and normalized to basal luminescence (0%) and the maximal effect of 2f-LIGRLO-NH₂ (100%) for the calculation of efficacy (E_{max}).

Metabolic stability. Metabolic stability of the test compounds was assessed in analogy to previously described protocols.¹⁰ The test compounds or a positive control (imipramine) were incubated (compound concentration of 20 μ M from a 10 mM stock solution in DMSO, total volume 500 μ L) with pooled male rat liver microsomes (Sprague-Dawley, Sigma-Aldrich, Germany) at a concentration of 0.5 mg microsomal protein/mL in Tris-MgCl₂ buffer (48 mM Tris, 4.8 mM MgCl₂, pH 7.4). Microsomal reactions were initiated by addition of 50 μ L of NADPH solution (Carl Roth, Germany, final concentration 1 mM) and carried out in polyethylene caps (Eppendorf, 1.5 mL) in a shaker at 37 °C, 350 rpm. At 0, 15, 30 and 60 min, 100 μ L were removed and 100 μ L of ice-cold CH₃CN (containing 10 μ M internal standard **14**) were added. Data were normalized using the internal standard and were plotted as % peak area of samples at t = 0 min (analysis of extracted ion chromatogram).

Plasma stability. In analogy to previously described protocols,⁶ compounds (10 mM stock solution in DMSO) were diluted to 100 μ M in PBS and 30 μ L of these dilutions were added to a mixture of rat plasma (150 μ L) and PBS (120 μ L) at 37 °C. At intervals of 0, 5, 15, 30, 60, 120, 180 and 240 min, 30 μ L were removed and 90 μ L of an ice-cold internal standard solution in CH₃CN was added (5 μ M internal standard **14**). Samples were centrifuged (13.000 rpm, 1 min) and the supernatant was analyzed by LC-MS. Data were

normalized using the internal standard and were plotted as % peak area of samples at $t = 0$ min (analysis of extracted ion chromatogram).

Cytotoxicity. Possible cytotoxic effects of ligand **5a** were studied in non-transfected HEK 293T cells employing the trypan blue exclusion test in analogy to previously described protocols.¹¹ In brief, cells were seeded at a density of 300.000 cells/mL in 12-well plates (Greiner) in complete growth medium and incubated with the test compounds (final concentration 1 μ M or 10 μ M concentration, diluted from a 10 mM stock solution prepared in DMSO) at 37 °C, 5% CO₂ for 24 h. The medium was removed and the cells were detached with 1 mL Versene (Invitrogen). Cells from three wells were collected and resuspended in growth medium, and 20 μ L of the resulting suspension were mixed with an equal amount of 0.4% trypan blue solution (Molecular Probes, Eugene, OR). Cell numbers and the fraction of dead cells were determined using a hemocytometer employing the automated Countess II FL cell counter (Invitrogen) and compared to control conditions (treated with a solution containing an equal amount of DMSO). For each condition, eight independent experiments were performed. Cell lysis in presence of 0.005% (w/v) digitonine (Sigma Aldrich) for 5 min was used as a positive control for cytotoxicity.

PAINS screening. All target compounds were converted into SMILES using ChemDraw 18.0 (PerkinElmer) and screened for pan assay interference and aggregation liability using the tools and standard filters¹² implemented in the ZINC 15 database.¹³ Results from the screening (Supplementary Table S1) indicate no liabilities for the target compounds.

Setup of MD simulations. The simulations are based on the PAR2 crystal structure in complex with the antagonist AZ8838 (PDB entry 5NDD)². The coordinates of the ligands were removed, and missing side chains completed utilizing UCSF Chimera to create the starting structure for modeling. MODELLER 9v4 was used to add the N-terminal residues 37 – 58, add missing residues in ECL3 and add 2 C-terminal residues up to Cys361. A palmitoyl group was added to Cys361 according to the UniProt entry of human PAR2. The C-terminus was capped with a methylamide group. Protonation states of titratable residues at pH 7.0 were calculated by means of the H⁺⁺ server ([http://biophysics.cs.vt.edu/H⁺⁺](http://biophysics.cs.vt.edu/H++))¹⁴.

The protein structure was aligned to the Orientation of Proteins in Membranes (OPM)¹⁵ structure of the PAR2 (PDB entry 5NDD). The complex was inserted into a solvated and pre-equilibrated membrane of dioleoyl-phosphatidylcholine (DOPC) lipids by means of the GROMACS tool g_membed¹⁶. Subsequently, water molecules were replaced by sodium and chloride ions to give a neutral system with 0.15 M NaCl. The final system dimensions were roughly 90 x 90 x 150 Å³, containing 221 lipids, 106 sodium ions, 116 chloride ions and about 27.000 water molecules.

Parameter topology and coordinate files were built up using the tleap module of AMBER16¹⁷ and subsequently converted into GROMACS input files. The general AMBER force field (GAFF)¹⁸ was used for DOPC molecules and ff14SB¹⁹ for the protein residues. The SPC/E water model²⁰ was applied.

Simulations were performed using GROMACS 2016.3²¹⁻²². The simulation systems were energy minimized and equilibrated in the NVT ensemble at 310 K for 1 ns followed by the NPT ensemble for 1 ns with harmonic restraints of 10.0 kcal·mol⁻¹ on protein and ligands. In the NVT ensemble the V-rescale thermostat was used. In the NPT ensemble the Berendsen barostat, a surface tension of 22 dyn·cm⁻¹, and a compressibility of 4.5×10^{-5} bar⁻¹ was applied. The system was further equilibrated for 18 ns with restraints on protein backbone. Here, the restraints were reduced in a stepwise fashion with 5.0 and 1.0 kcal·mol⁻¹, respectively. 100 ns of unrestrained molecular dynamics simulation were performed to further equilibrate the system. Simulations were performed using periodic boundary conditions and time step of 2 fs with bonds involving hydrogen constrained using LINCS. Long-range electrostatic interactions were computed using particle mesh Ewald (PME)²³ method with interpolation of order 4 and FFT grid spacing of 1.6 Å. Non-bonded interactions were cut off at 12.0 Å.

Metadynamics simulations of N-terminal signaling sequence binding. Metadynamics simulations were performed in order to obtain a binding mode of the trypsin activated N-terminus to the receptor itself. The simulations were performed based on the recently described protocol by Saleh and coworkers to determine ligand binding modes at GPCR²⁴. In brief, we used a combination of the well-tempered metadynamics (WT)²⁵⁻²⁶ and funnel-shaped walls. A metadynamics-history-dependent bias was applied along the z component of the distance between the center of mass of the C α atoms of Phe155^{3.32}, Tyr156^{3.33} and Ser333^{7.42}, representing the

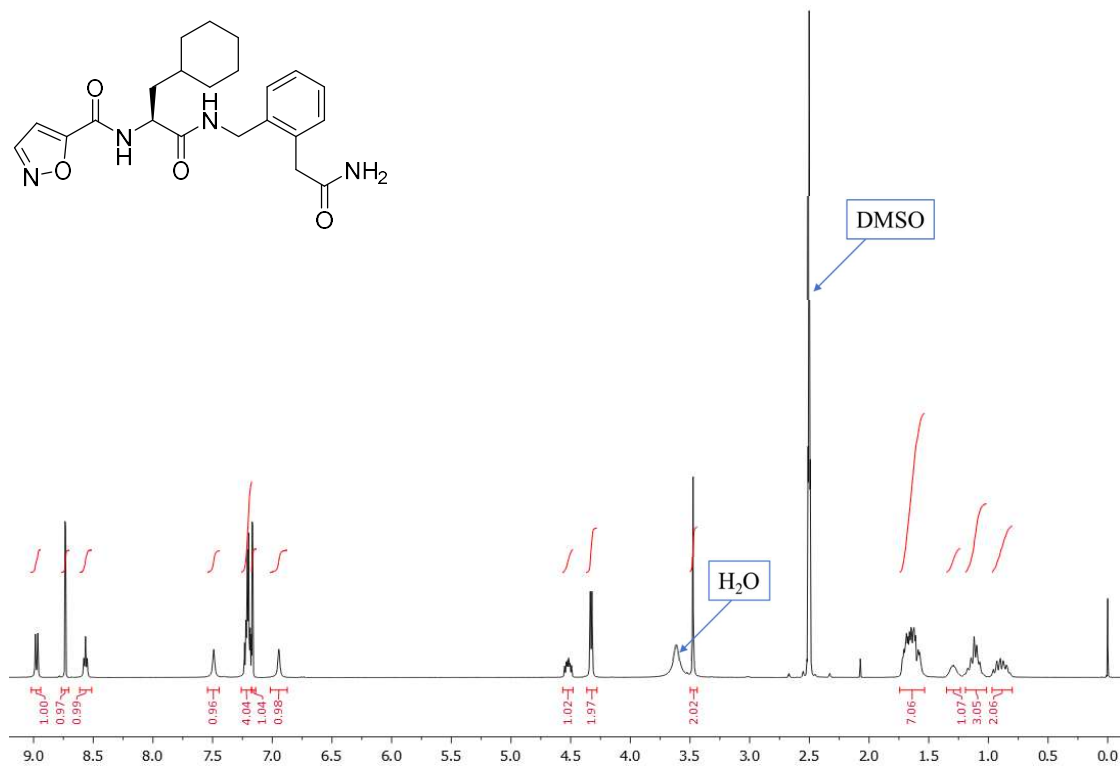
center of the receptor, and center of mass of the N-terminal Ser37. This distance was used as the single collective variable. The funnel restraint was applied to the relative position on the xy plane to ensure better sampling for the relevant region. Gaussian hills with an initial height of $0.48 \text{ kcal}\cdot\text{mol}^{-1}$ applied every 1 ps were used. The hill width was chosen to be 1 Å. The Gaussian functions were rescaled in the WT scheme using a bias factor of 20. The free energies were calculated using the sum_hills function of the PLUMED plugin²⁷. The lowest energy binding mode was equilibrated in a 1 μs long unrestrained MD simulation.

Molecular Docking. Docking studies were performed using the PAR2 model of Kennedy et al.³ and the equilibrated model of the N-terminal bound PAR2 proposed by the metadynamics simulations. For the latter, the N-terminal sequence SLIGKVD of the receptor was removed to expose the cavity used for docking. The peptide sequence SLIGKV was removed from the PAR2 model of Kennedy et al.³ for the same purpose. The 3D coordinates of the compounds were created and optimized using Avogadro²⁸, an open-source molecular builder and visualization tool (Version 1.2.0). Docking was performed using AutoDock Vina²⁹ applying a search space of $20 \times 20 \times 20 \text{ \AA}$ and an exhaustiveness value of 32. Twenty conformations of each ligand were obtained and inspected manually.

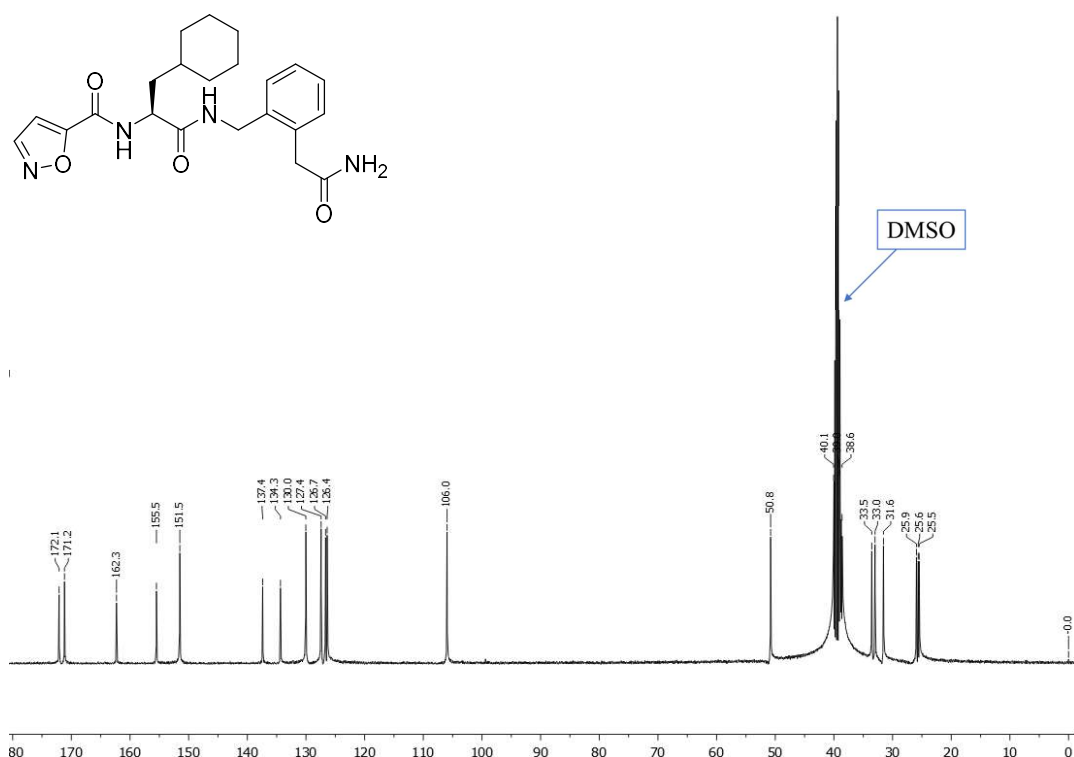
Subsequently, the selected ligand-receptor complexes of **4b** (IK109), **5a** (IK187) and **2** were submitted to an energy minimization using the PMEMD module of the AMBER18 program package³⁰. The general AMBER force field 2 (GAFF2)³⁰ was used for small molecules and ff14SB¹⁹ for protein residues. Parameters for **4b** (IK109), **5a** (IK187) and **2** were assigned using antechamber³⁰. Structures of the ligands were optimized by means of Gaussian 16³¹ at the B3LYP/6-31G* level and charges were calculated at the HF/6-31G* level of theory. Atom point charges were assigned according to the RESP procedure described in literature²⁰. No formal charge was assigned to the ligands. The minimization protocol includes 500 steps of steepest descent minimization, followed by 4500 steps of conjugate gradient minimization. The energy minimizations were carried out in a water box with periodic boundary conditions and a non-bonded cutoff of 10.0 Å. Visualization was performed using the PyMOL Molecular Graphics System, Version 2.1.1 (Schrödinger, LLC).

Supplementary Data. ^1H and ^{13}C NMR spectra of the key compounds.

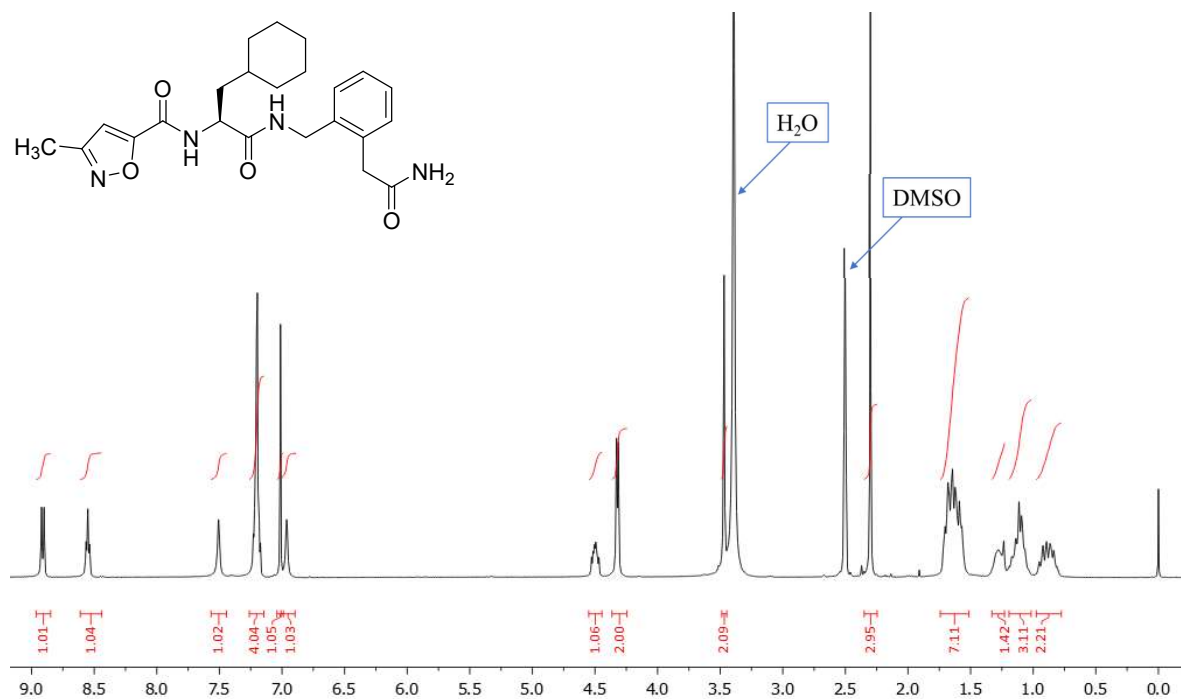
4b, ^1H -NMR, DMSO-d₆, 400 MHz



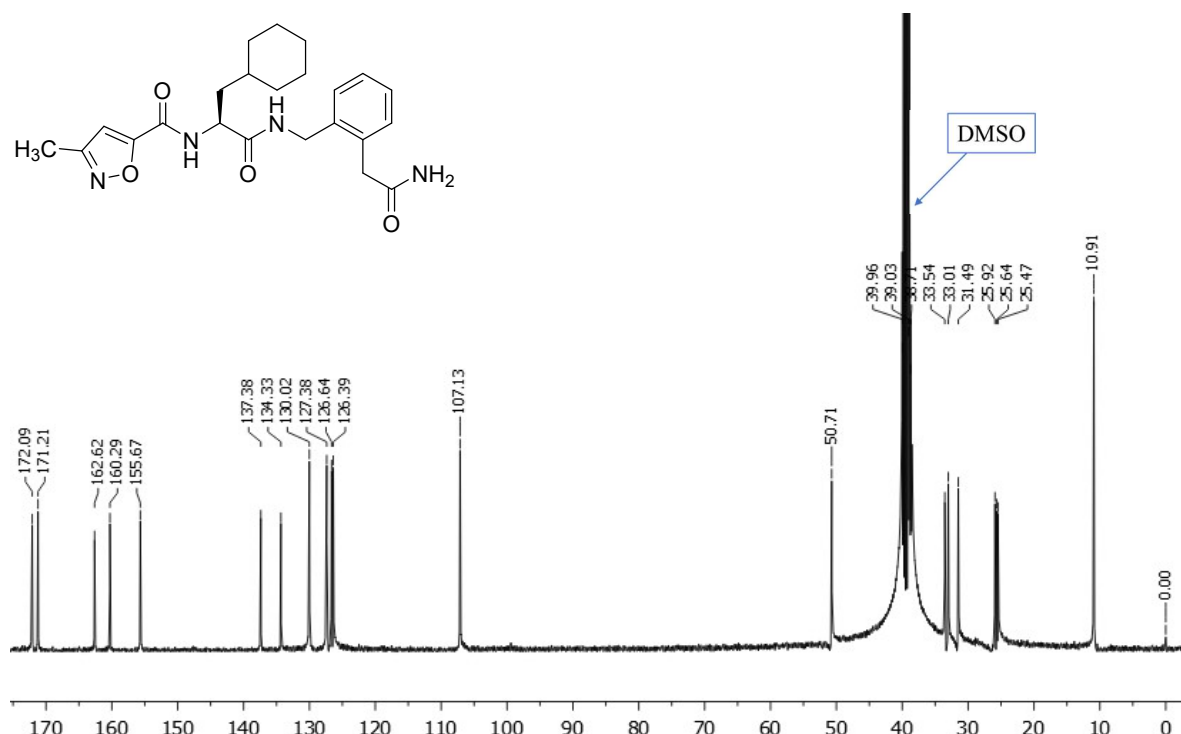
4b, ^{13}C -NMR, DMSO-d₆, 101 MHz



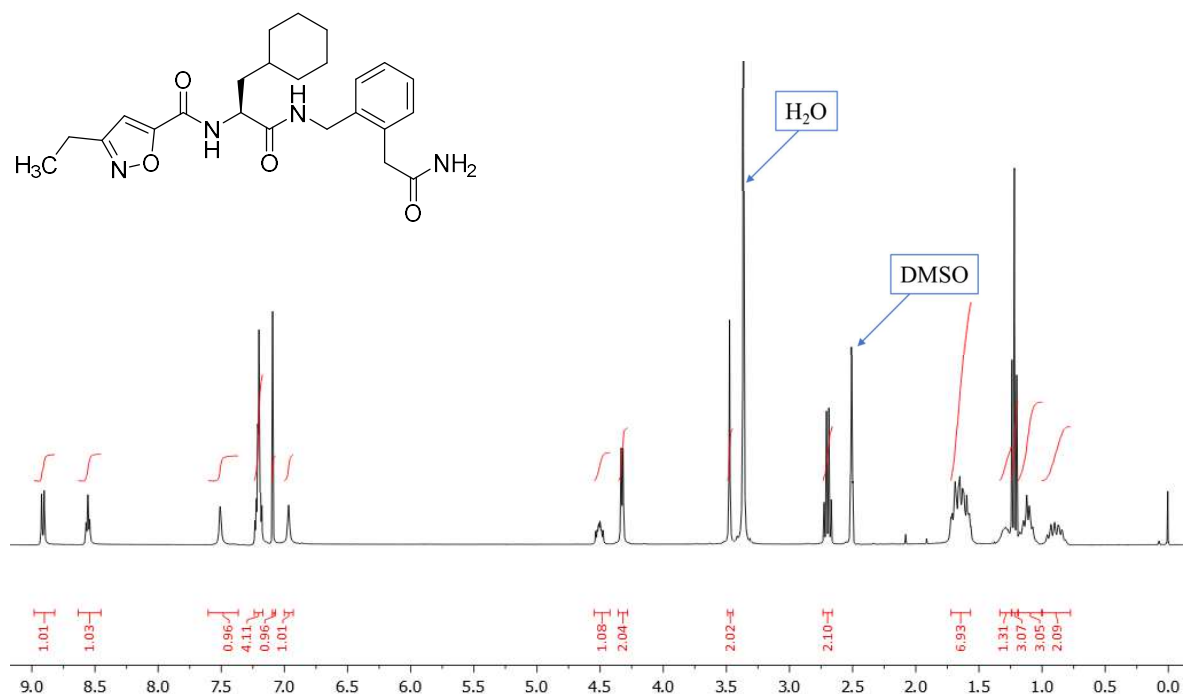
5a, ^1H -NMR, DMSO- d_6 , 400 MHz



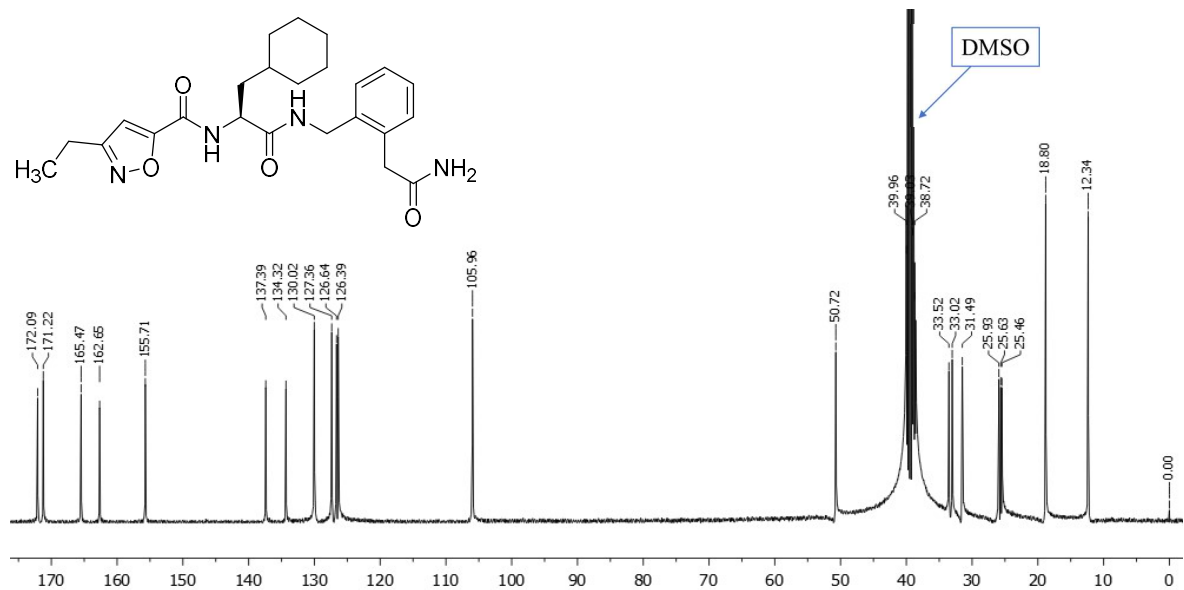
5a, ^{13}C -NMR, DMSO- d_6 , 101 MHz



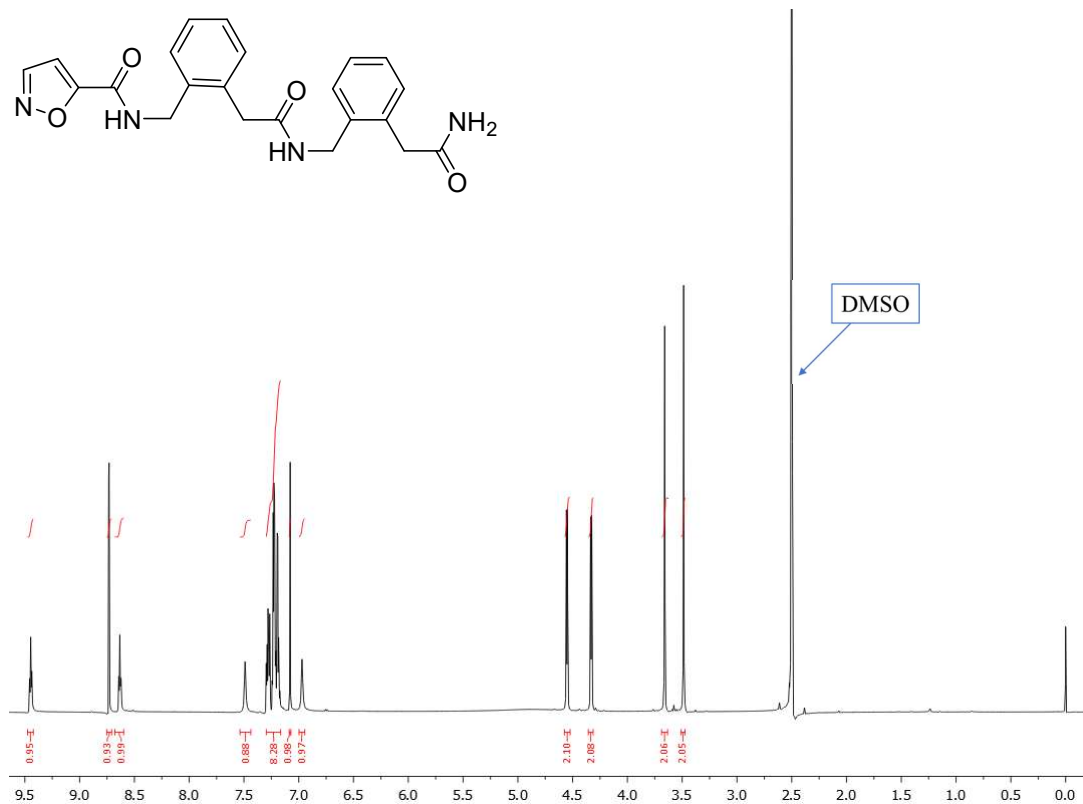
5b, ^1H -NMR, DMSO- d_6 , 400 MHz



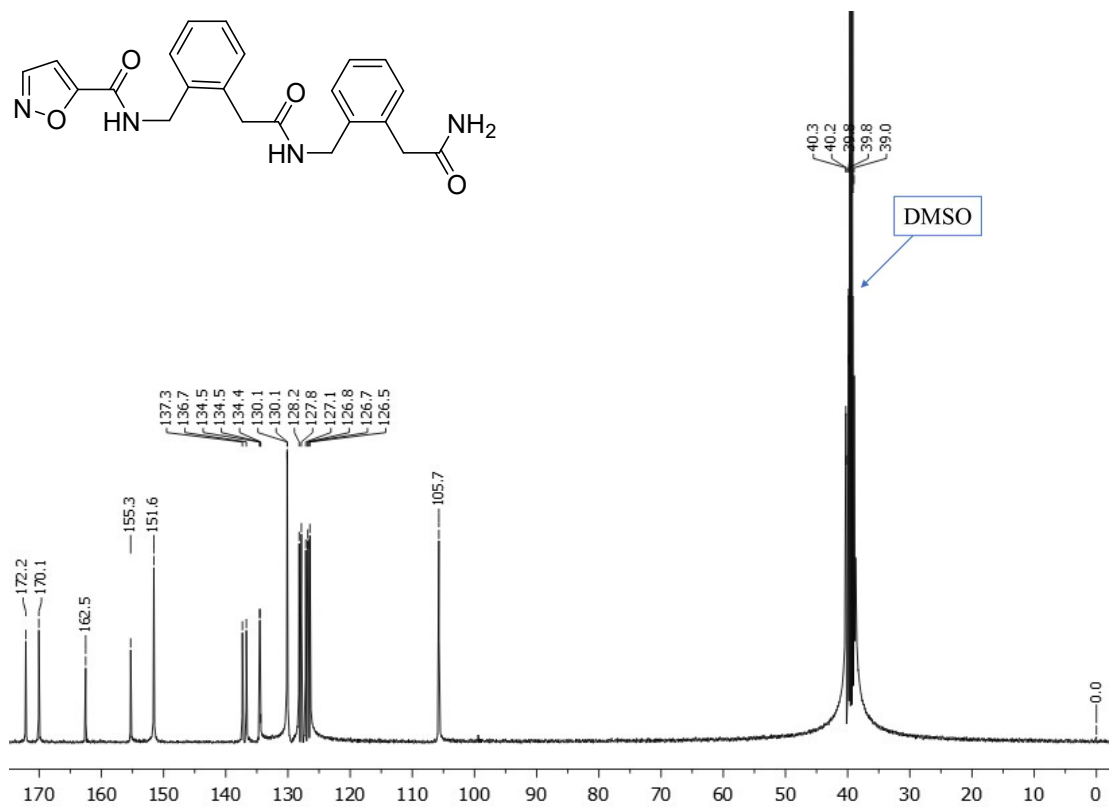
5b, ^{13}C -NMR, DMSO- d_6 , 101 MHz



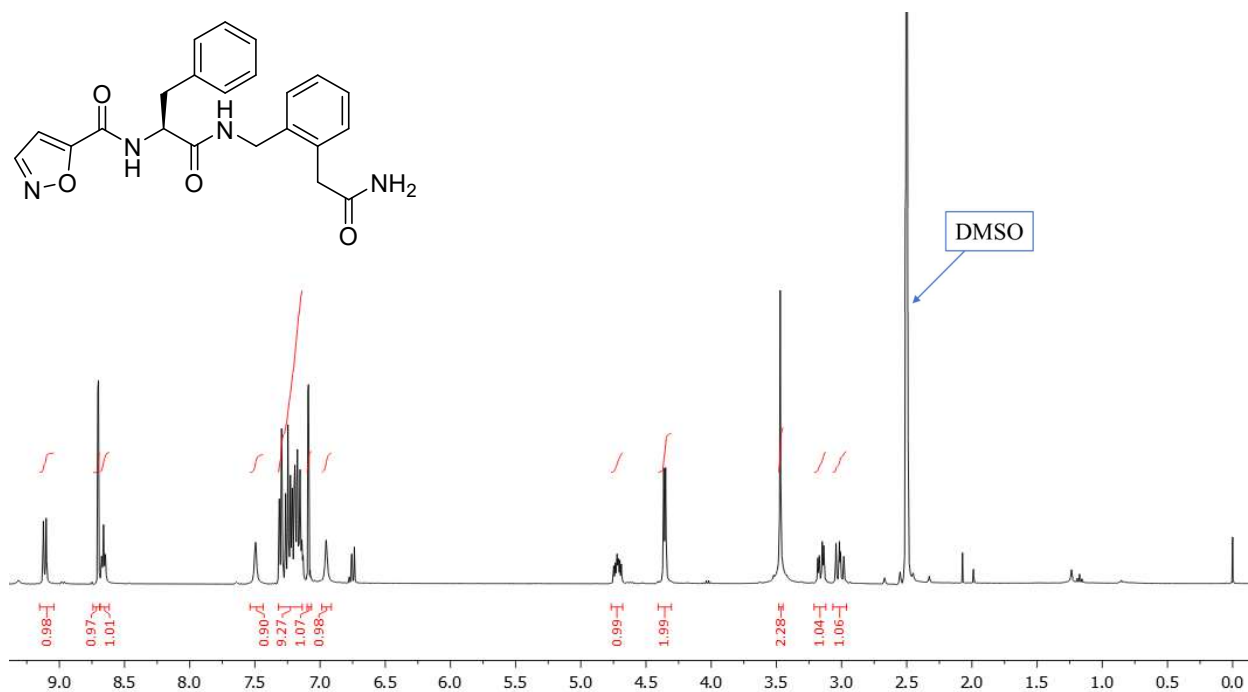
6, $^1\text{H-NMR}$, DMSO- d_6 , 600 MHz



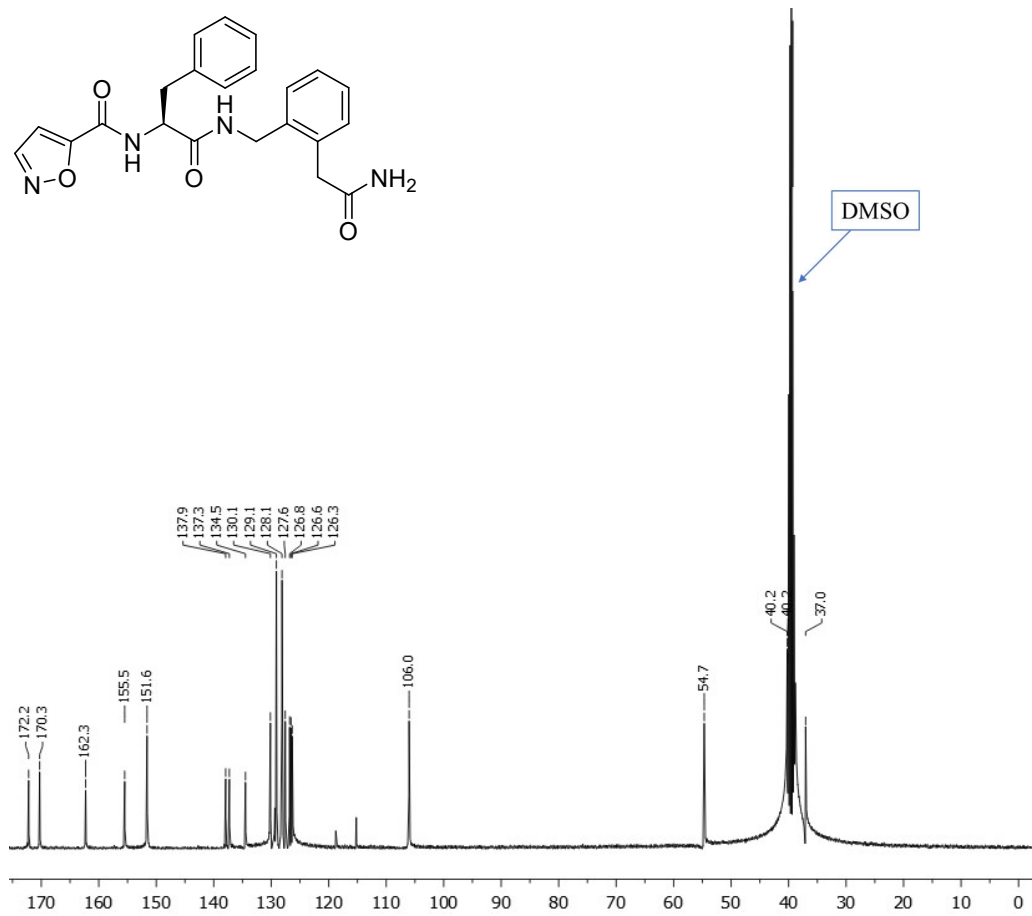
6, ^{13}C -NMR, DMSO- d_6 , 101 MHz



7, ^1H -NMR, DMSO- d_6 , 400 MHz

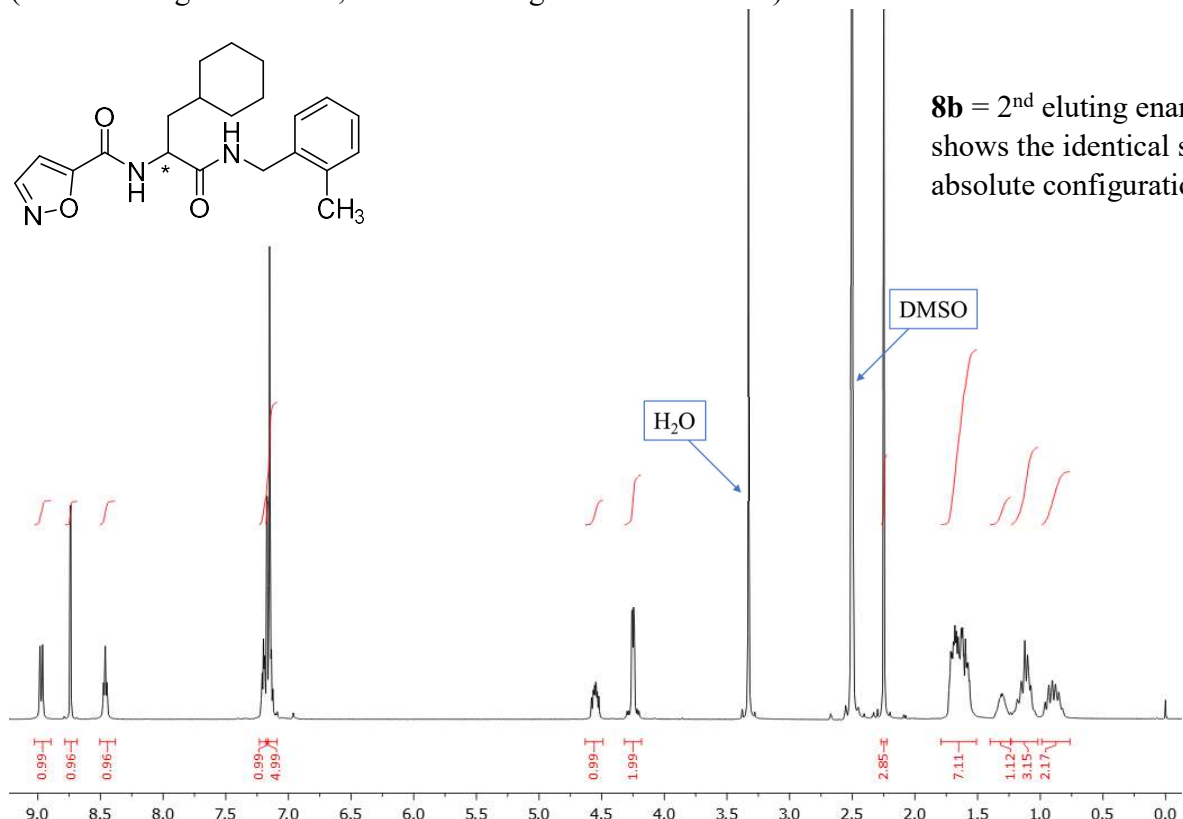


7, ^{13}C -NMR, DMSO- d_6 , 101 MHz



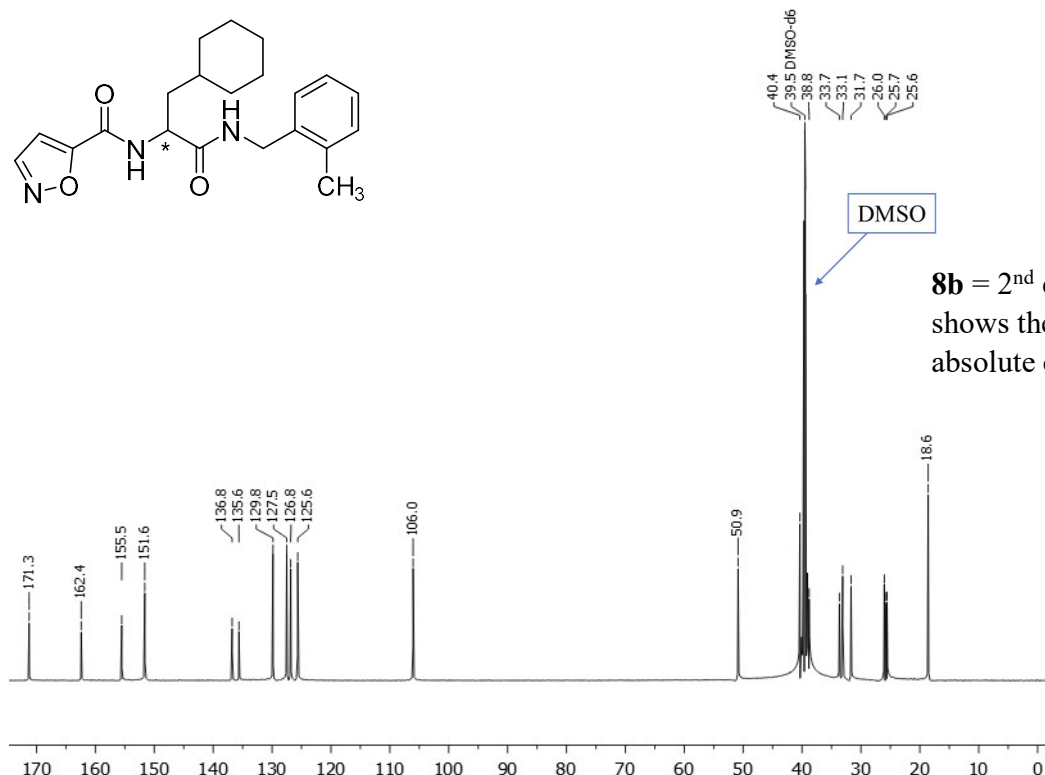
8a, ^1H -NMR, DMSO- d_6 , 400 MHz

(= first eluting enantiomer, absolute configuration not known)



8a, ^{13}C -NMR, DMSO- d_6 , 151 MHz

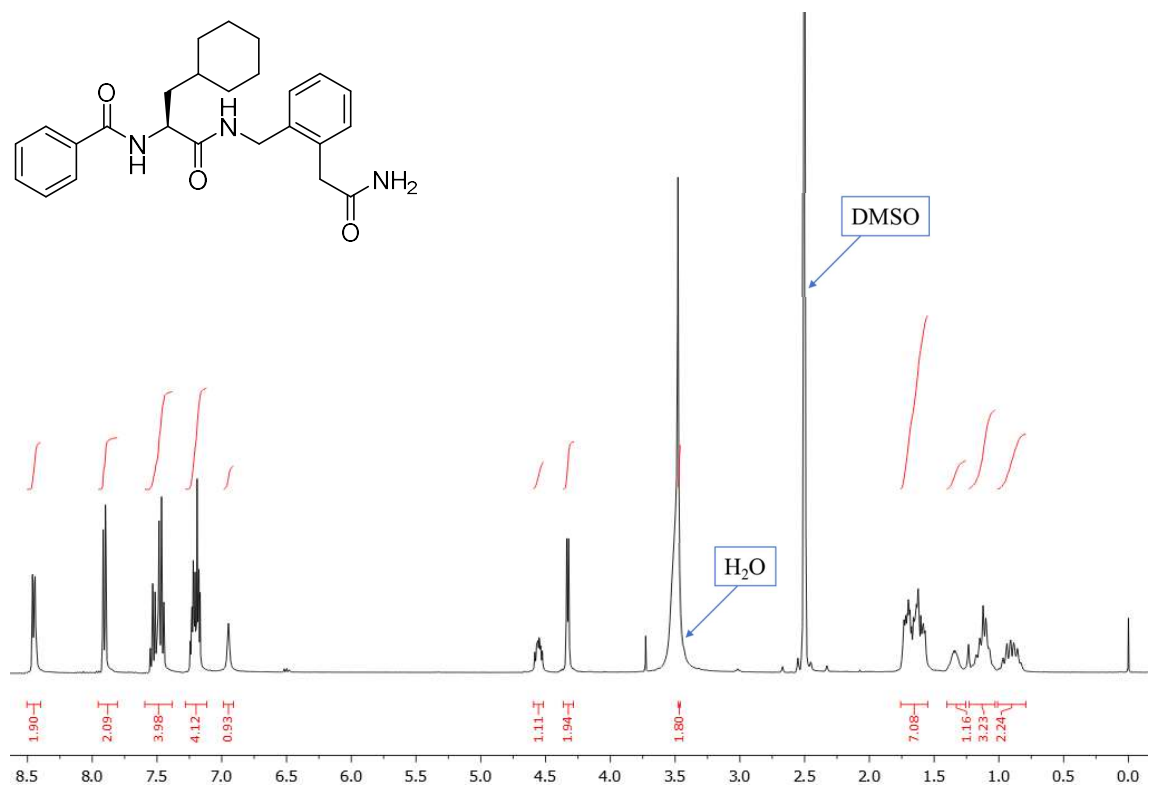
(= first eluting enantiomer, absolute configuration not known)



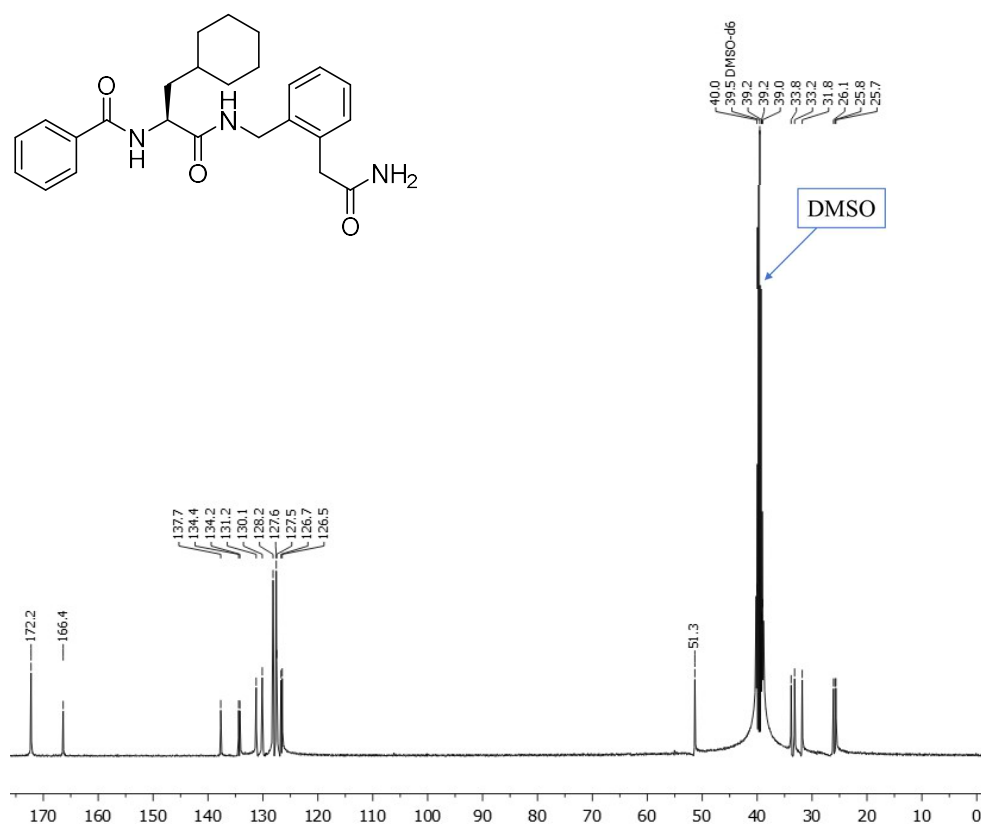
8b = 2nd eluting enantiomer:

shows the identical spectrum as **8a**,
absolute configuration is not known

9, ^1H -NMR, DMSO- d_6 , 400 MHz

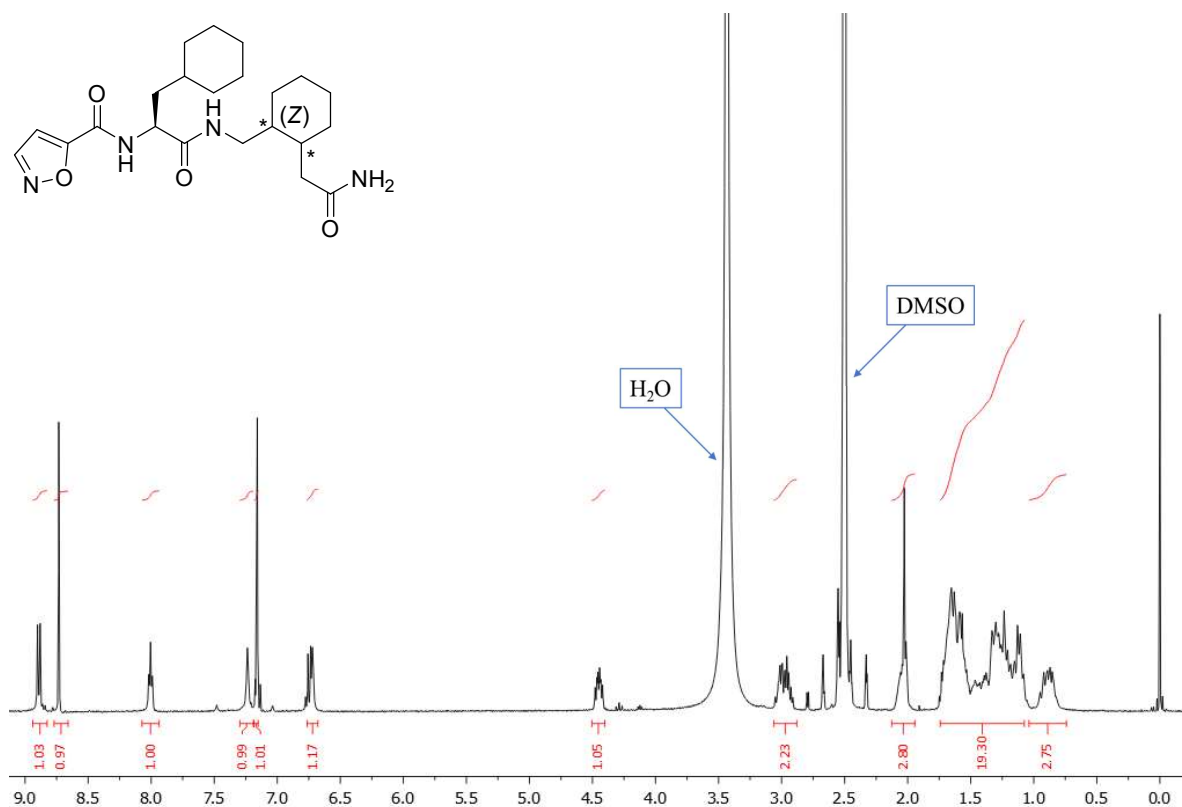


9, ^{13}C -NMR, DMSO- d_6 , 101 MHz



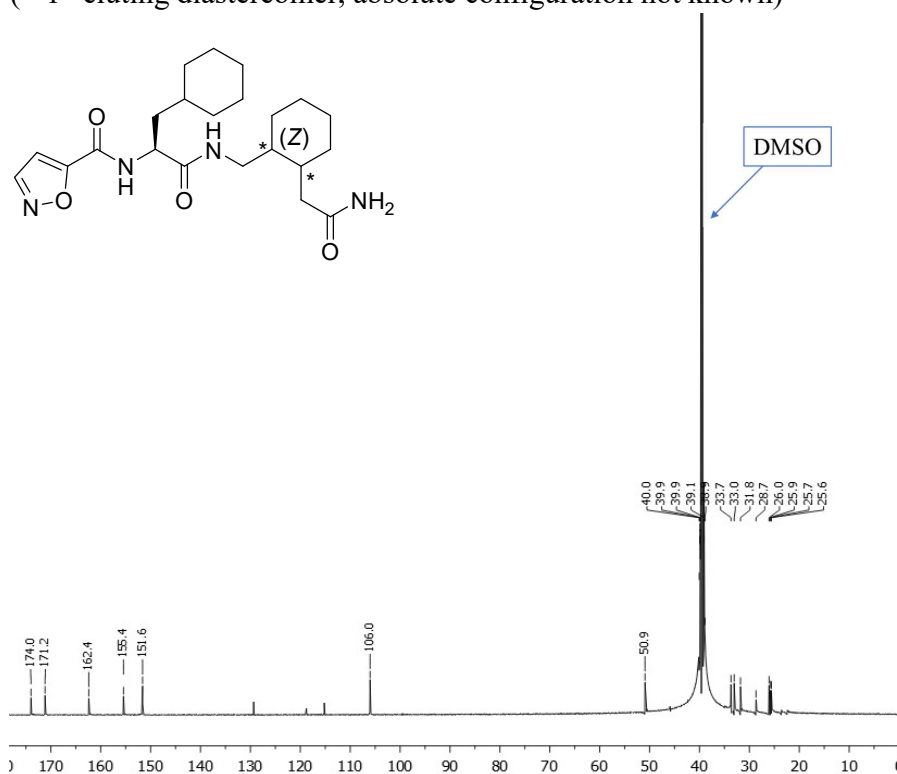
10a, ^1H -NMR, DMSO- d_6 , 400 MHz

(= 1st eluting diastereomer, absolute configuration not known)



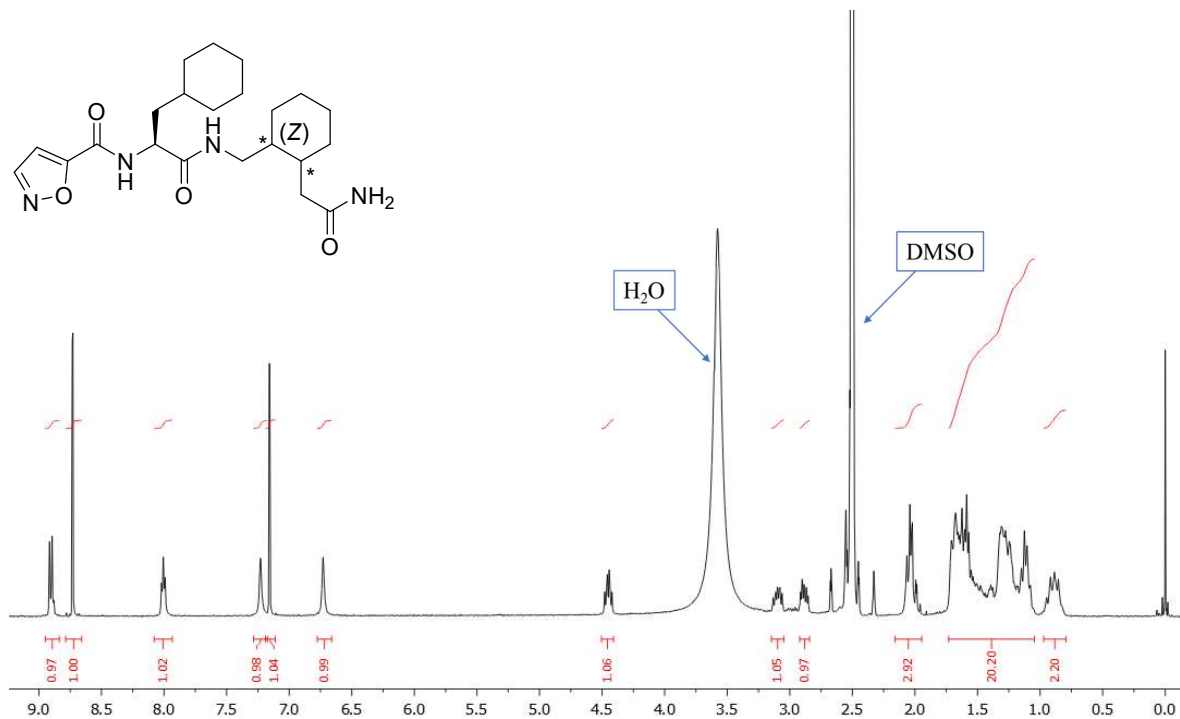
10a, ^{13}C -NMR, DMSO- d_6 , 151 MHz

(= 1st eluting diastereomer, absolute configuration not known)



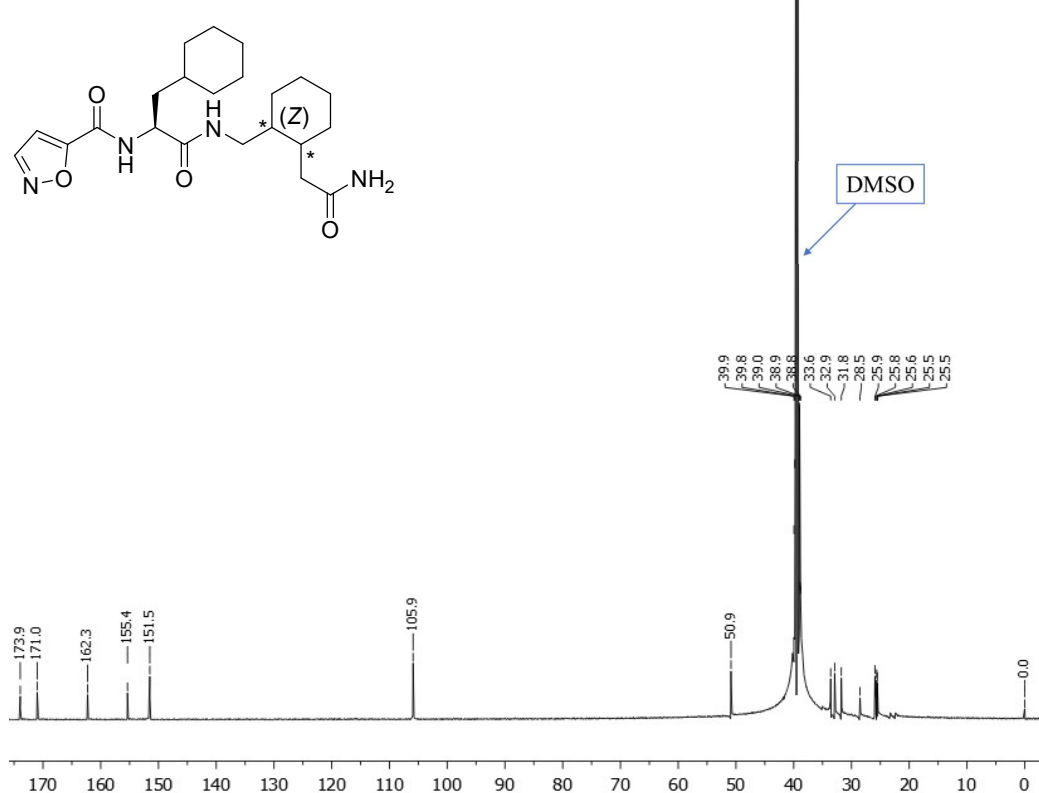
10b, ^1H -NMR, DMSO- d_6 , 400 MHz

(= 2nd eluting diastereomer, absolute configuration not known)

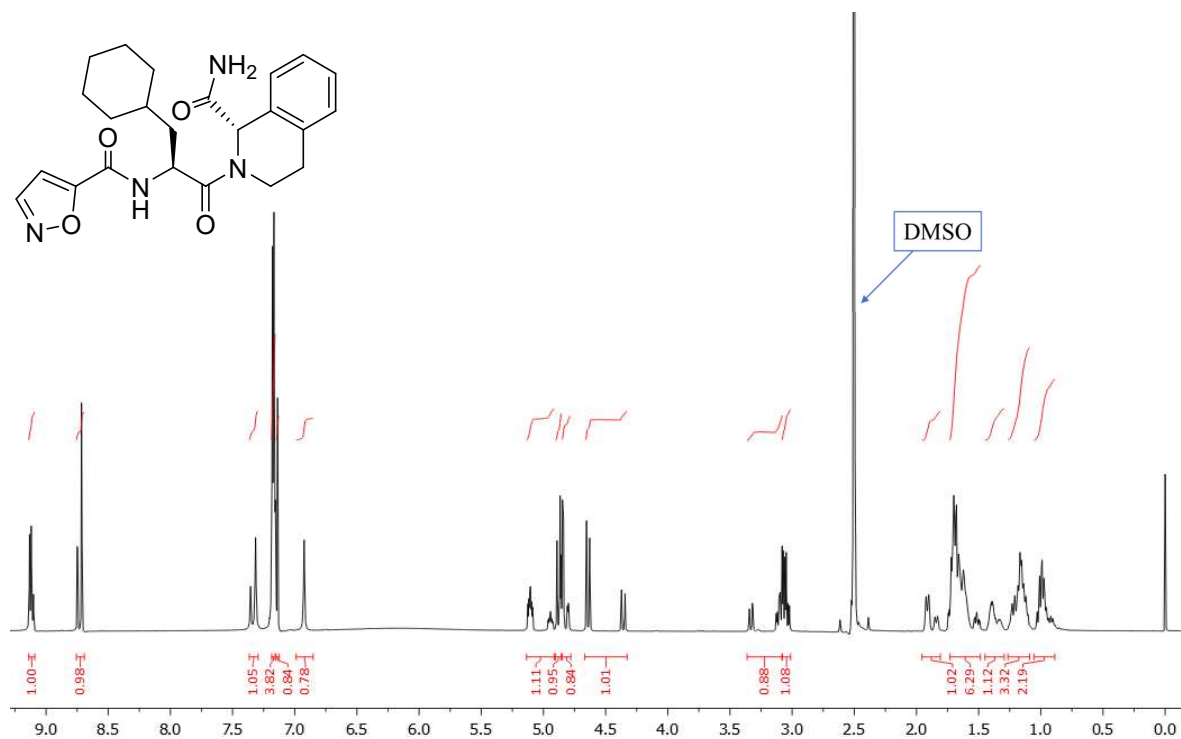


10b, ^{13}C -NMR, DMSO- d_6 , 151 MHz

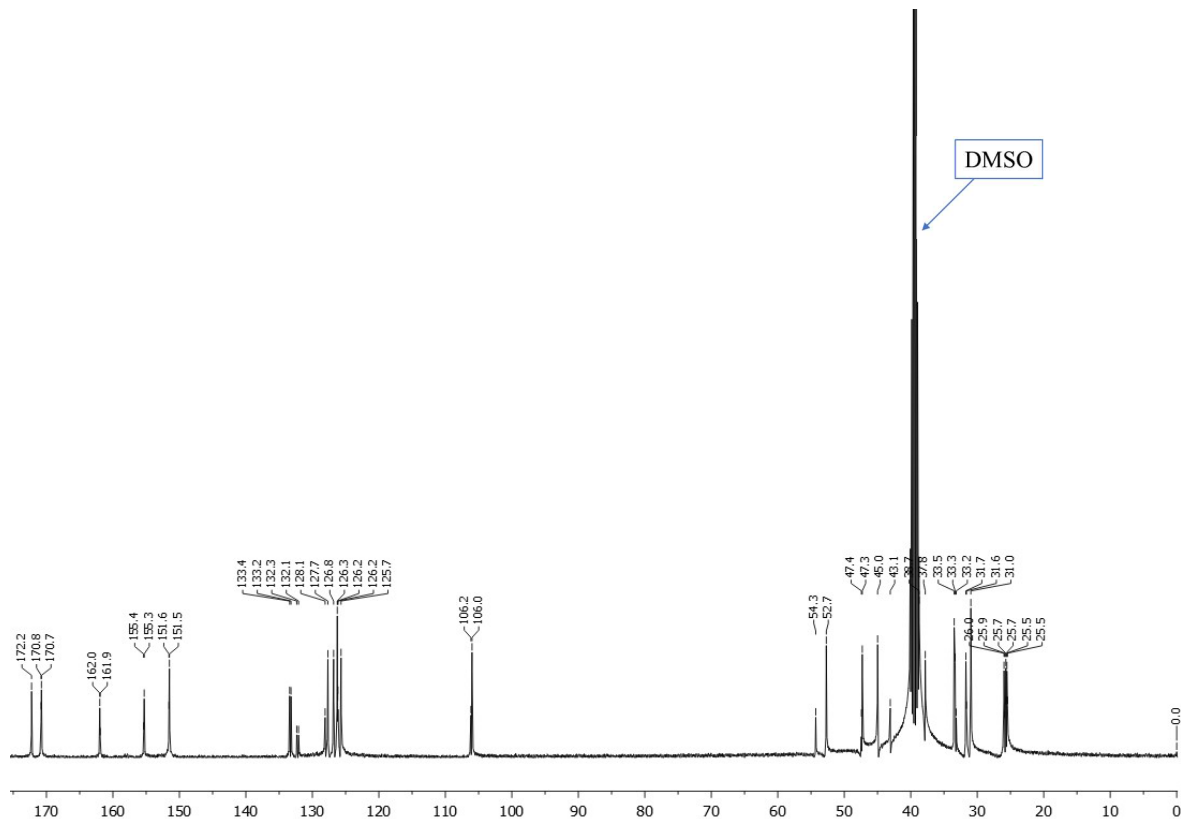
(= 2nd eluting diastereomer, absolute configuration not known)



11, ^1H -NMR, DMSO- d_6 , 600 MHz

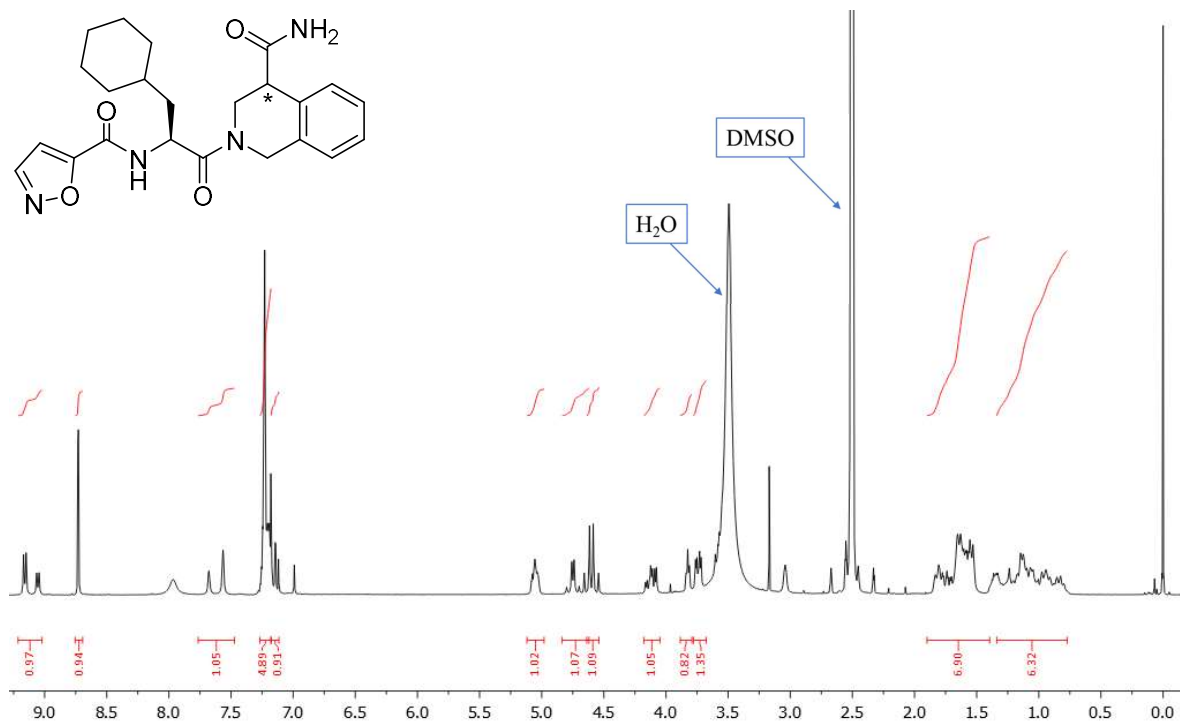


11, ^{13}C -NMR, DMSO- d_6 , 101 MHz



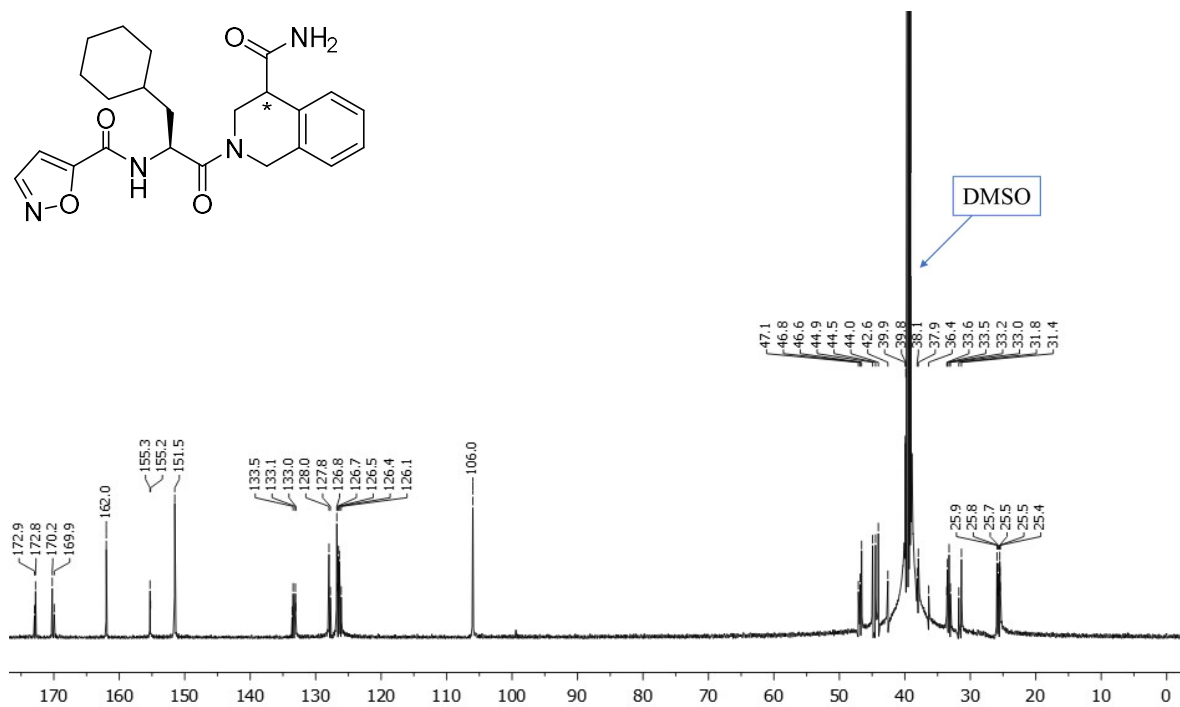
12a, ^1H -NMR, DMSO- d_6 , 400 MHz

(= 1st eluting diastereomer, absolute configuration not known)



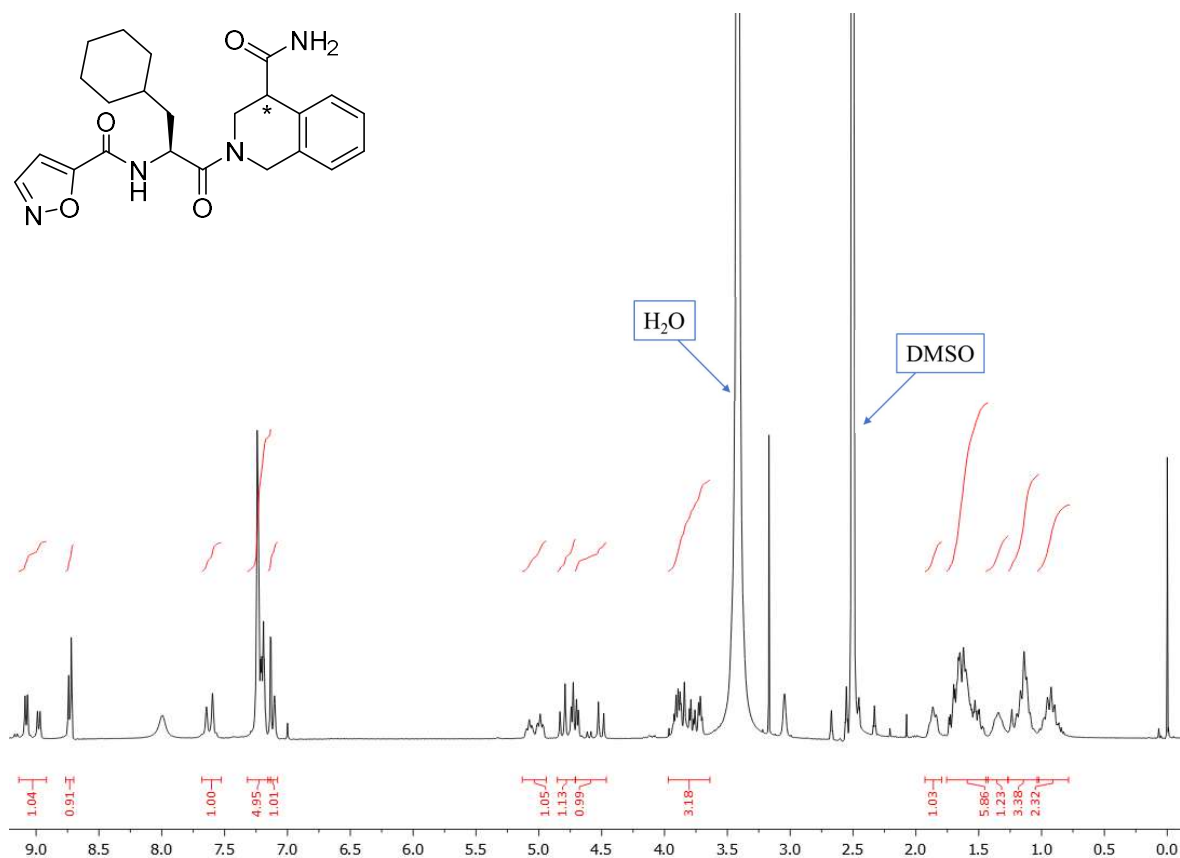
12a, ^{13}C -NMR, DMSO- d_6 , 151 MHz

(= 1st eluting diastereomer, absolute configuration not known)



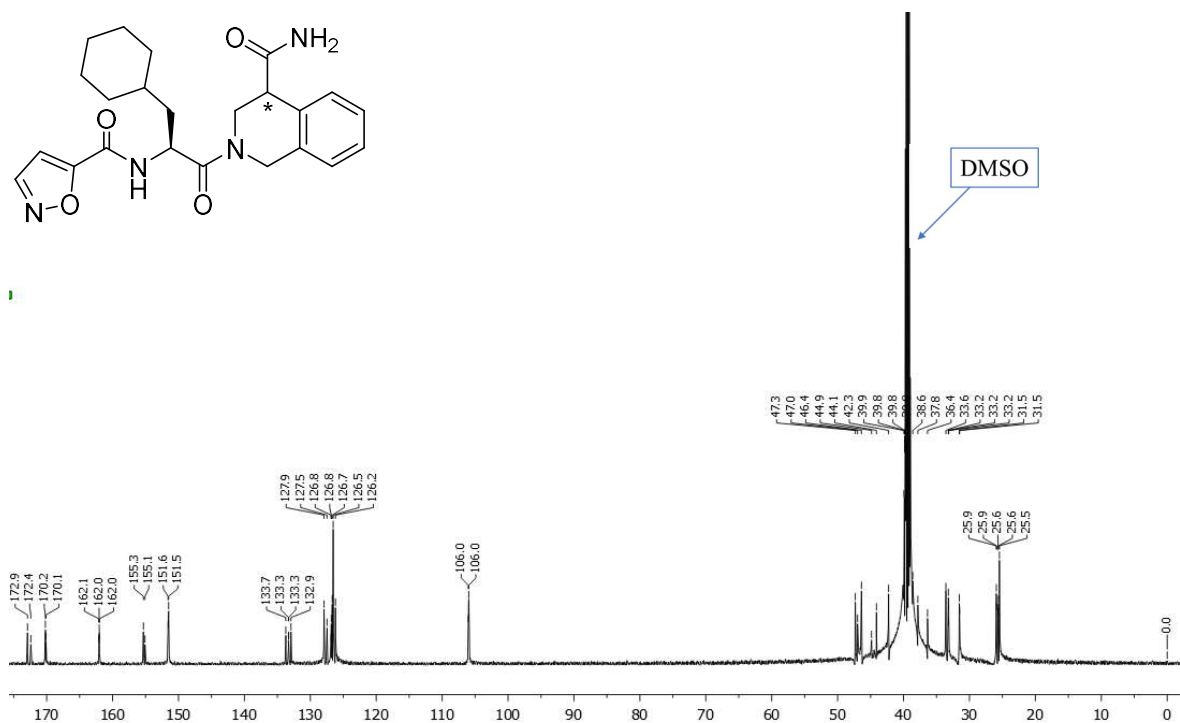
12b, ^1H -NMR, DMSO- d_6 , 400 MHz

(= 2nd eluting diastereomer, absolute configuration not known)

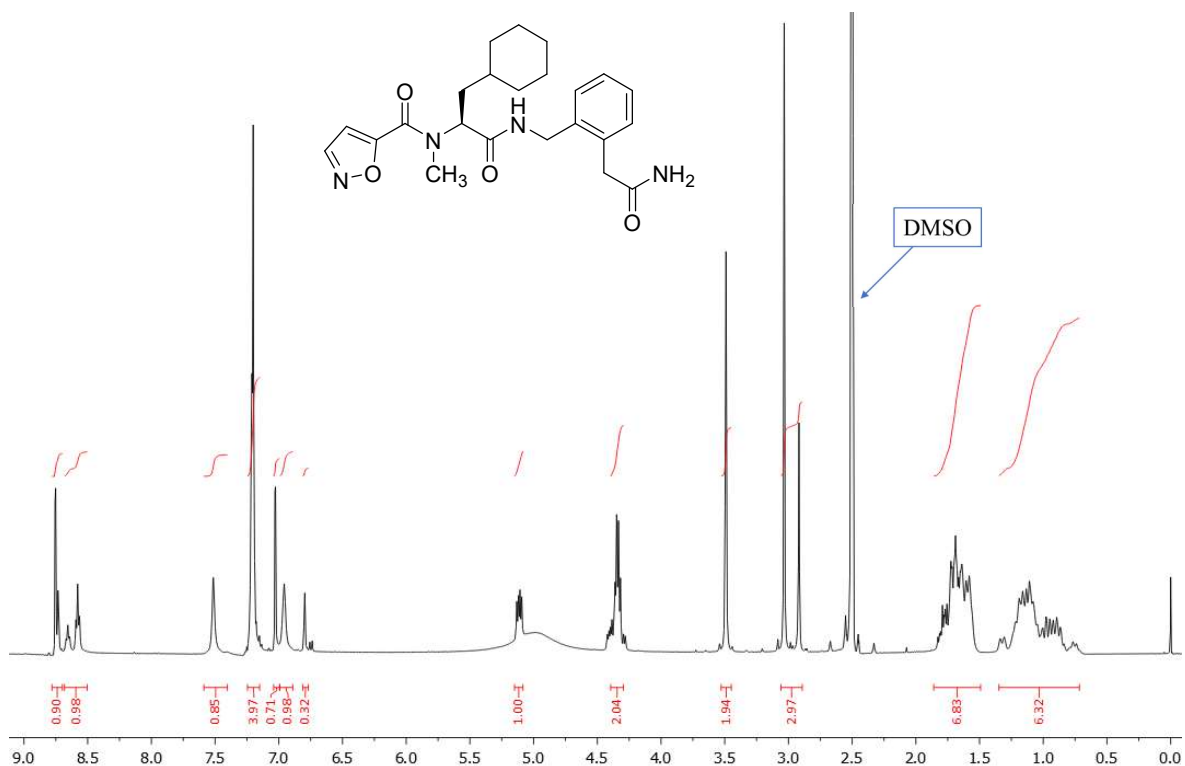


12b, ^{13}C -NMR, DMSO- d_6 , 151 MHz

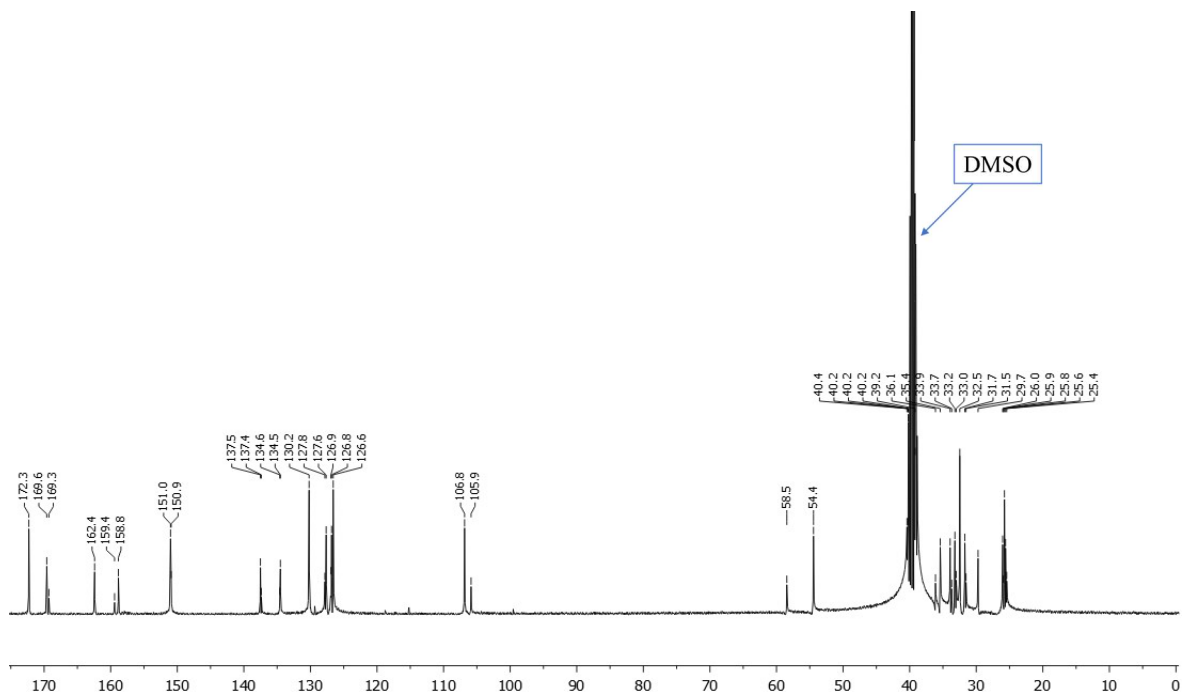
(= 2nd eluting diastereomer, absolute configuration not known)



13, ^1H -NMR, DMSO- d_6 , 400 MHz

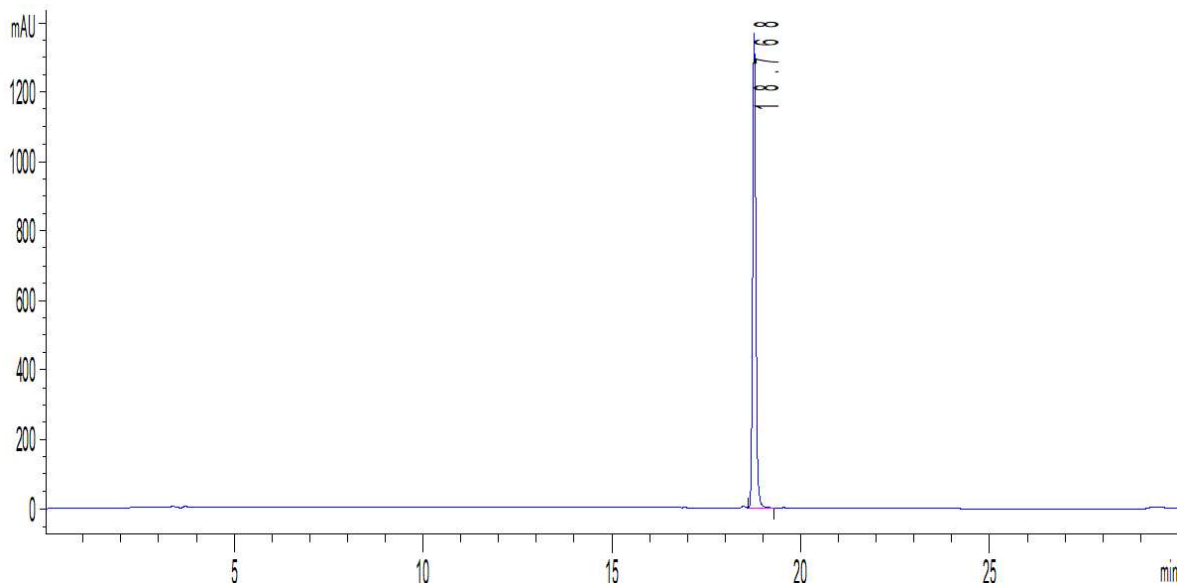


13, ^{13}C -NMR, DMSO- d_6 , 101 MHz

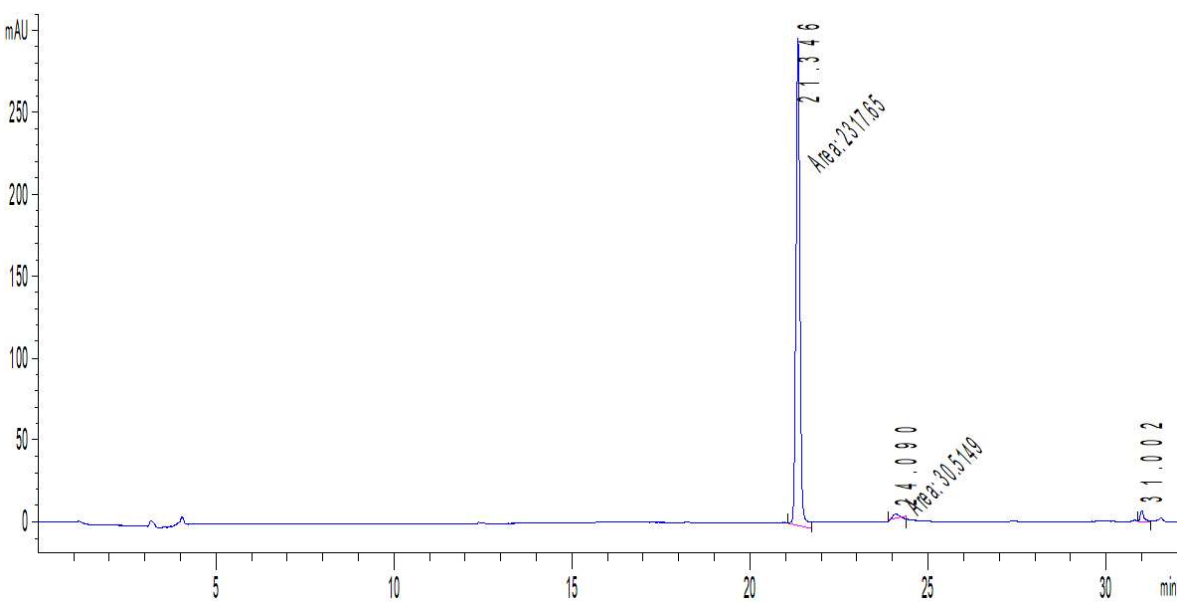


Supplementary Data. HPLC traces of the key compounds.

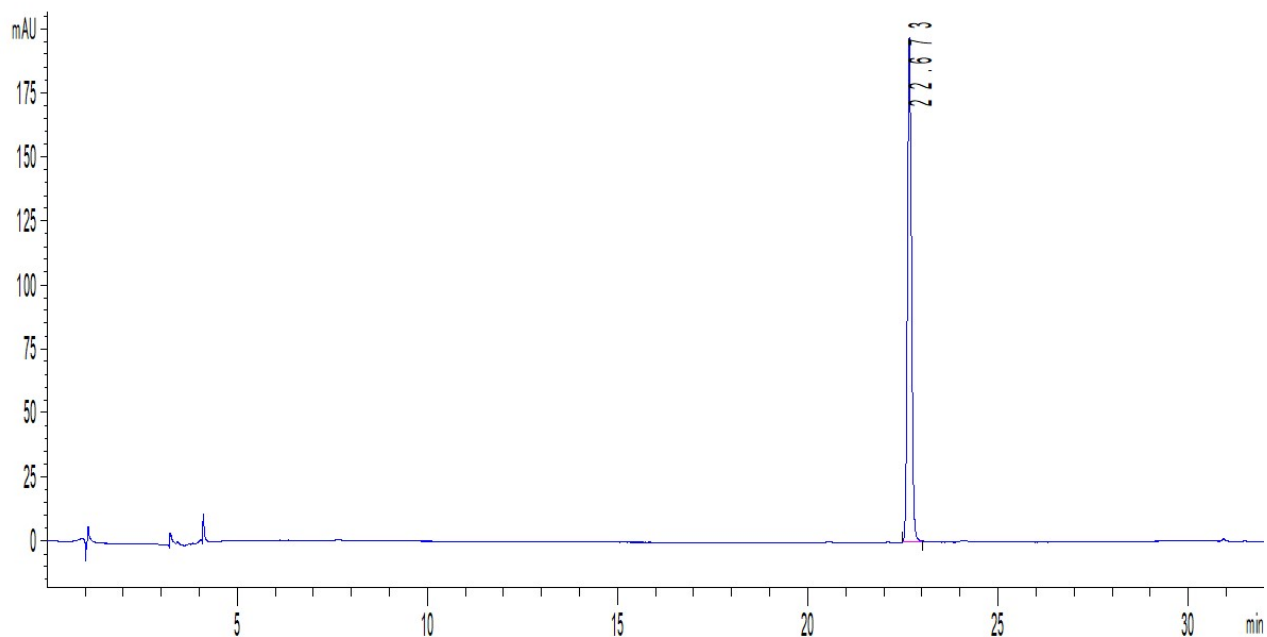
4b, HPLC system 1, $\lambda = 254$ nm



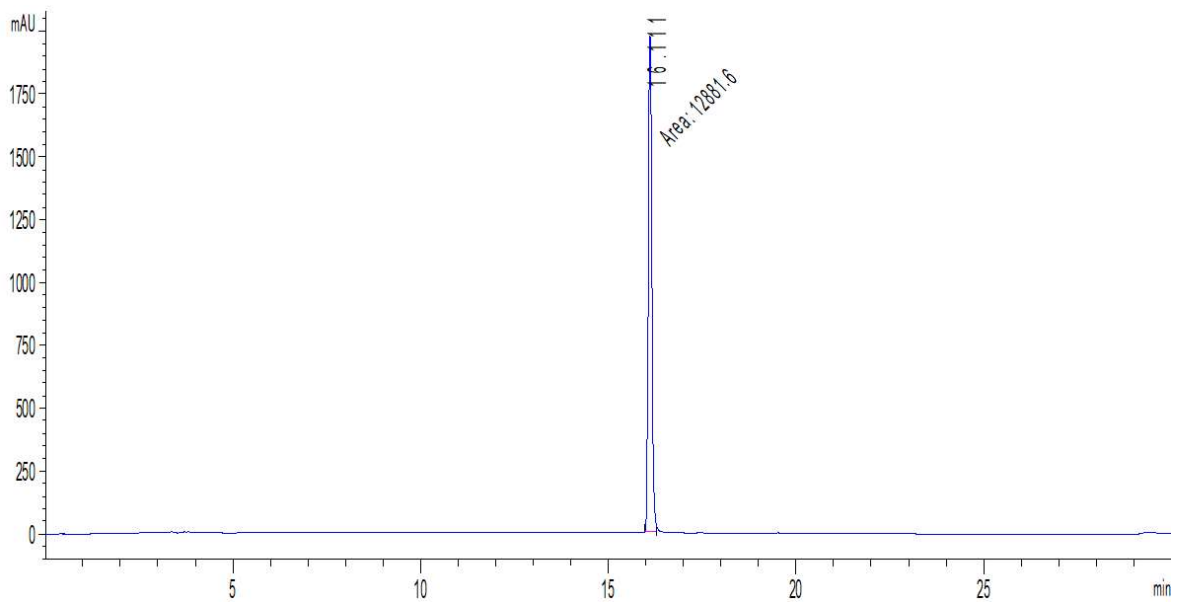
5a, HPLC system 2, $\lambda = 254$ nm



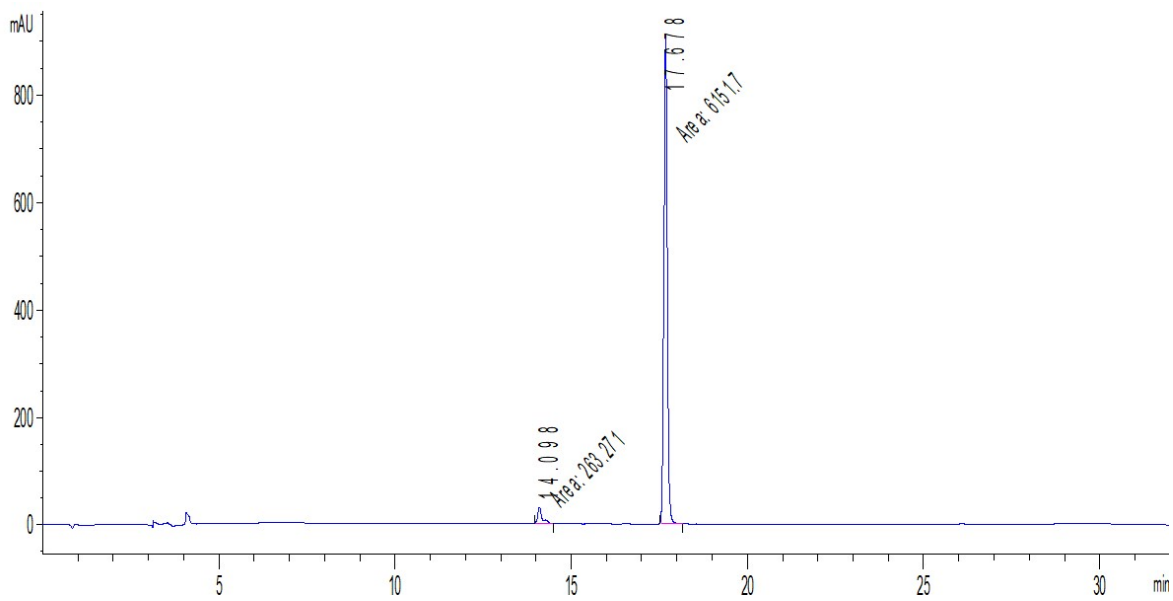
5b, HPLC system 2, $\lambda = 254$ nm



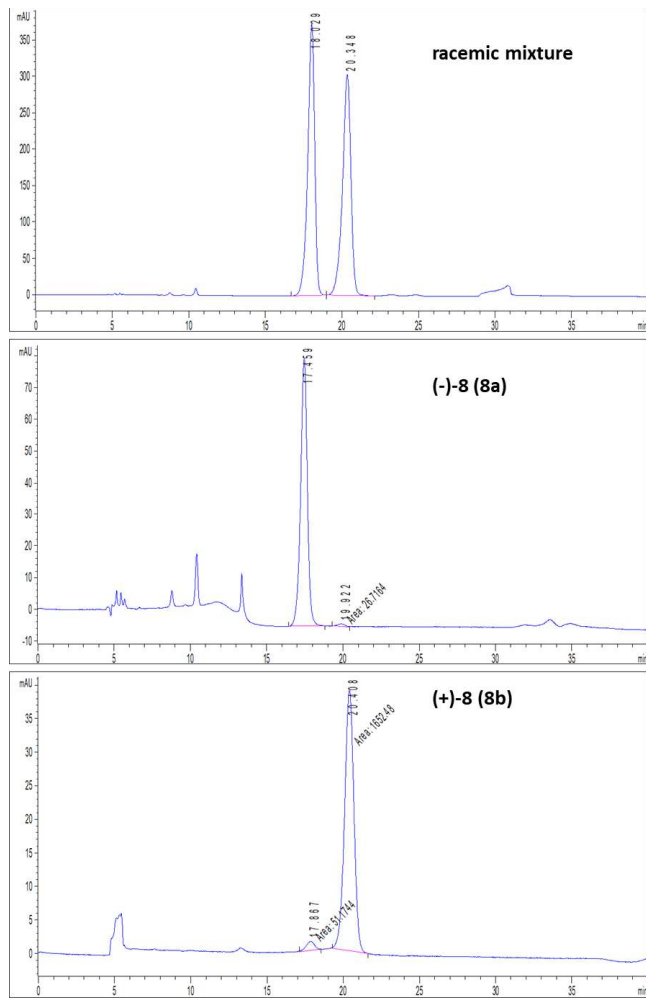
6, HPLC system 1, $\lambda = 254$ nm



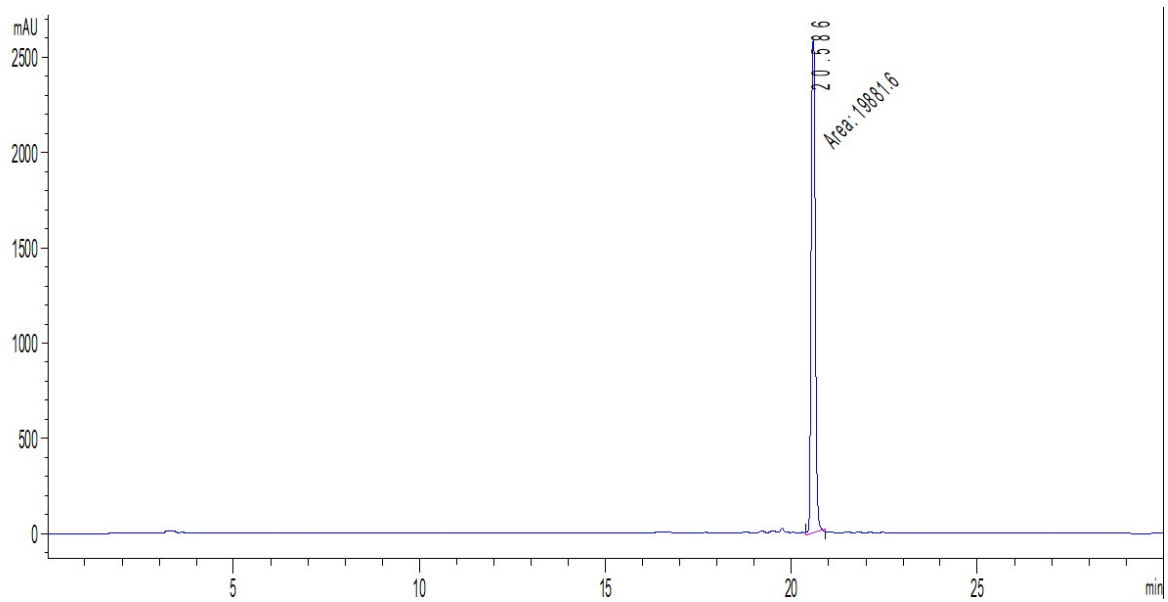
7, HPLC system 1, $\lambda = 254$ nm



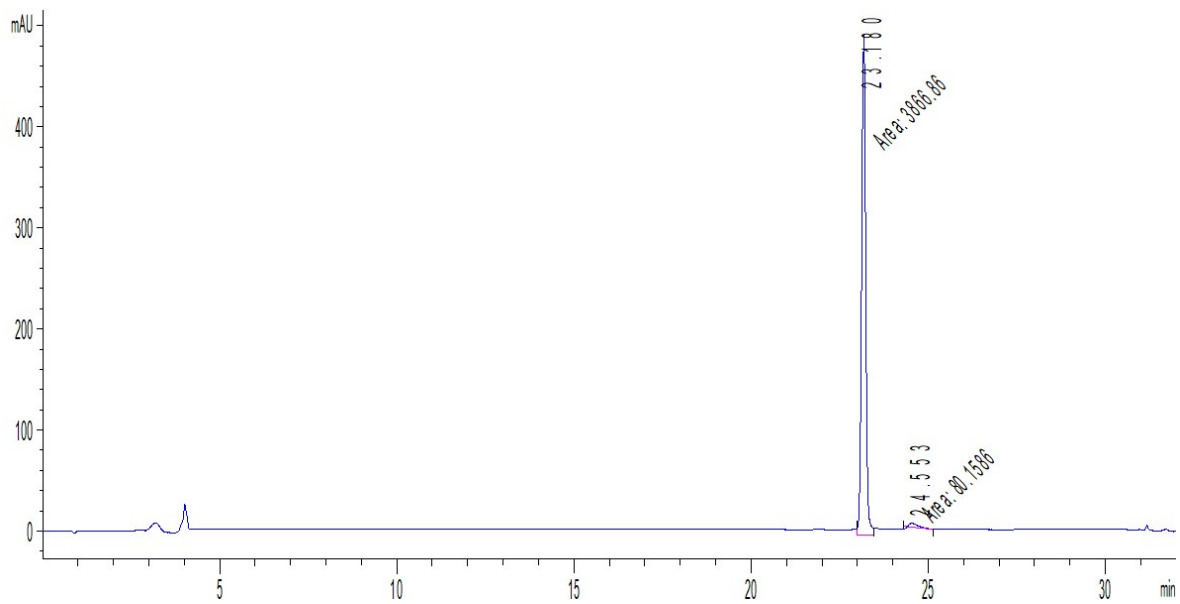
8a/8b, chiral HPLC, hexane/isopropanol + 0,1% EDA, $\lambda = 254$ nm



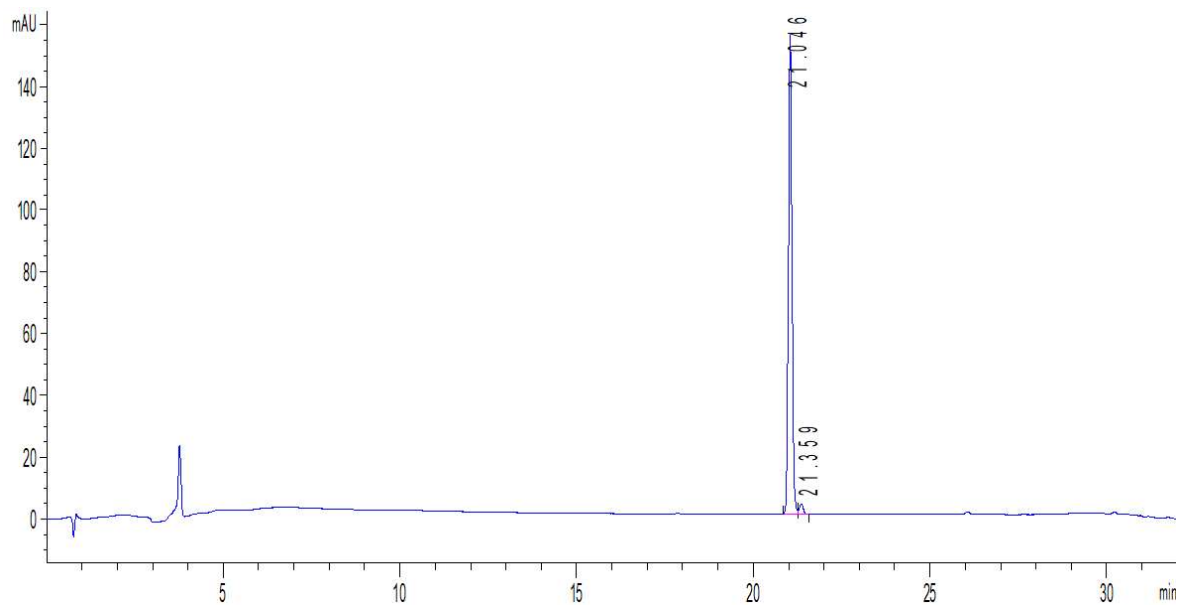
8a/8b, HPLC system 1, $\lambda = 254$ nm



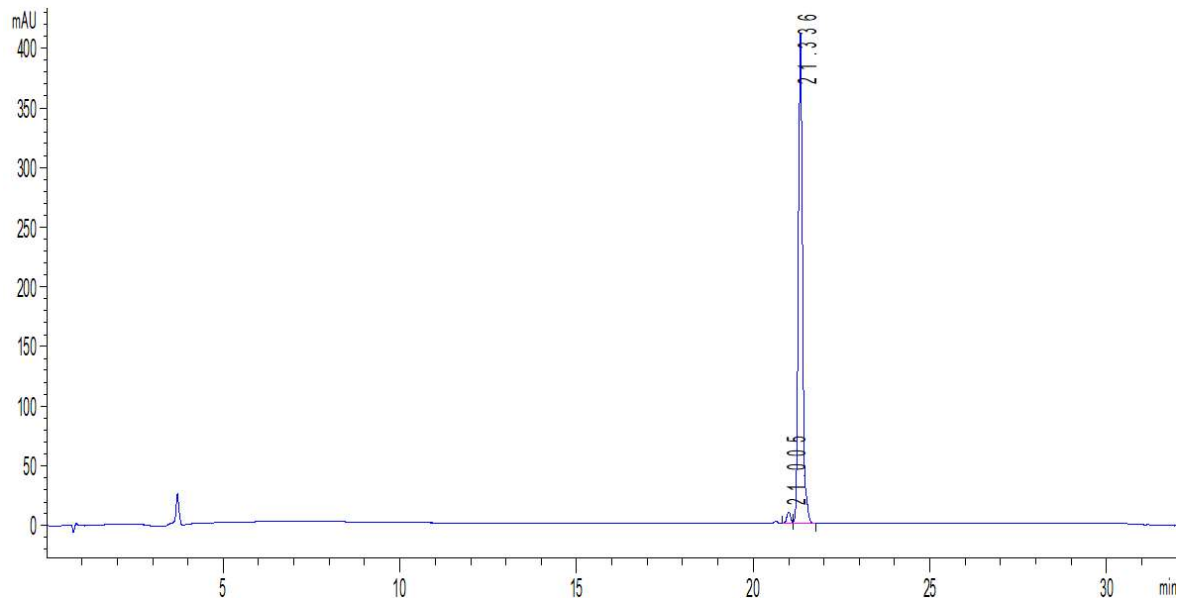
9, HPLC system 2, $\lambda = 254$ nm



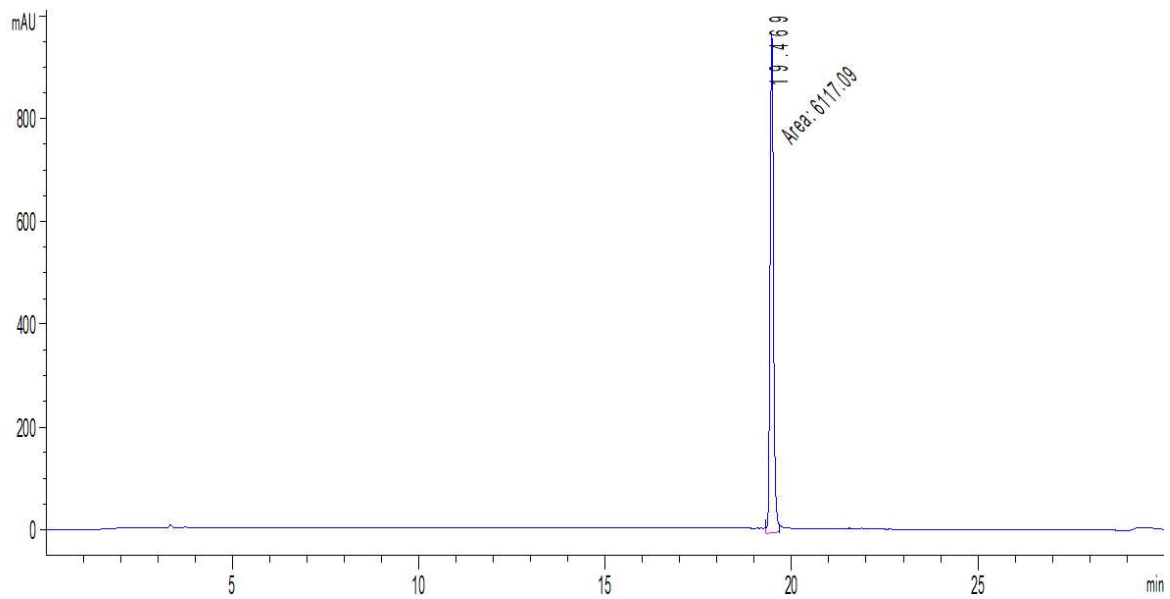
10a, HPLC system 2, $\lambda = 254$ nm



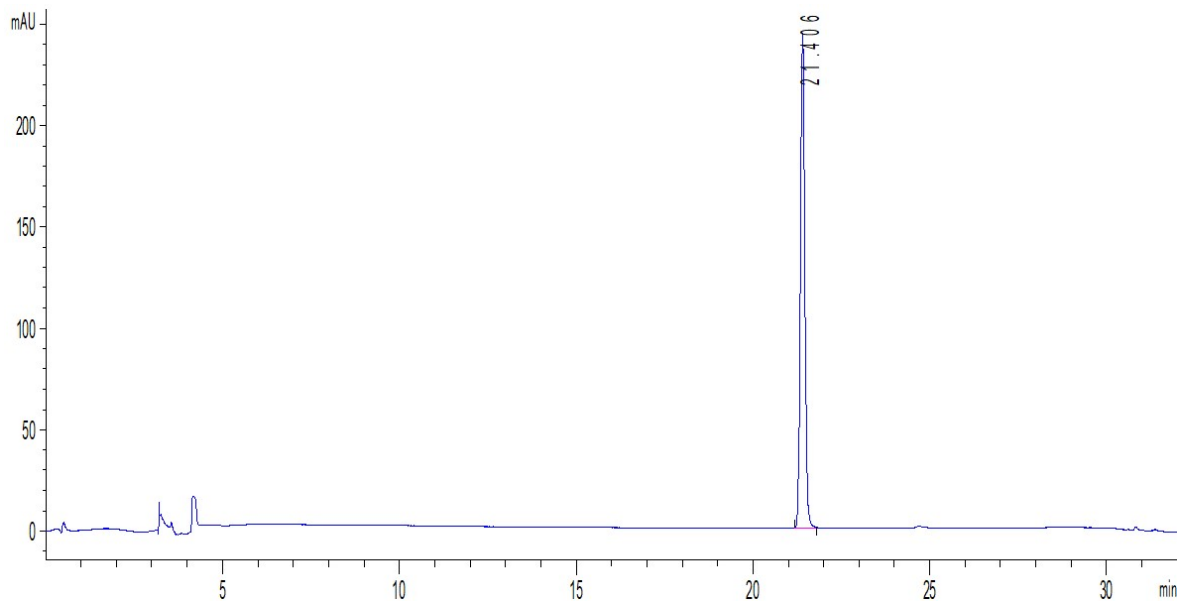
10b, HPLC system 2, $\lambda = 254$ nm



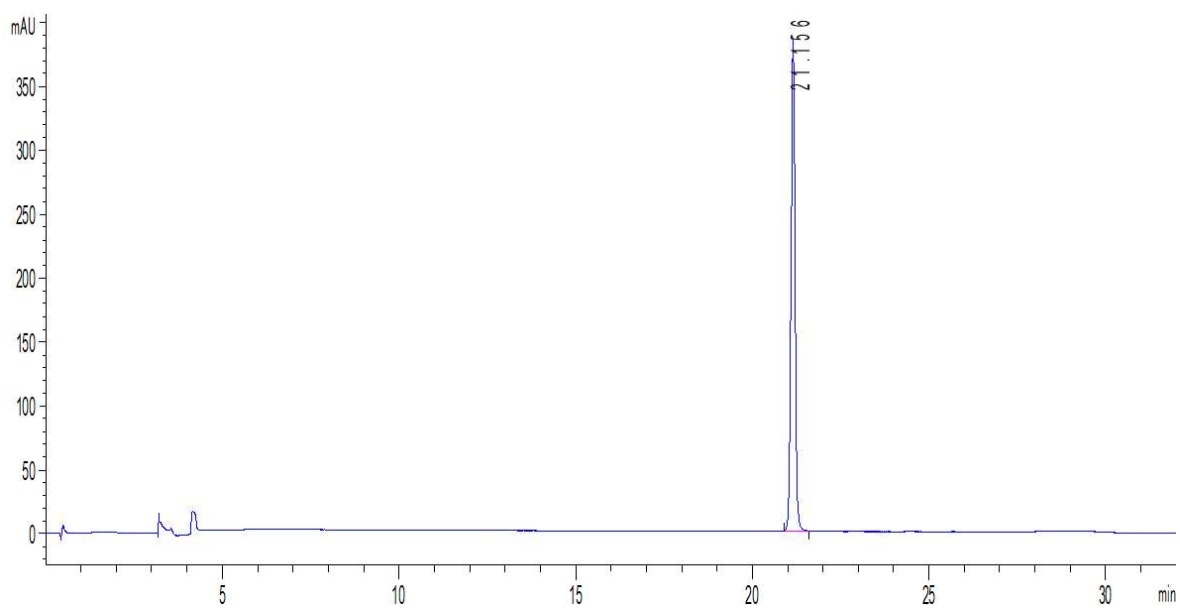
11, HPLC system 1, $\lambda = 254$ nm



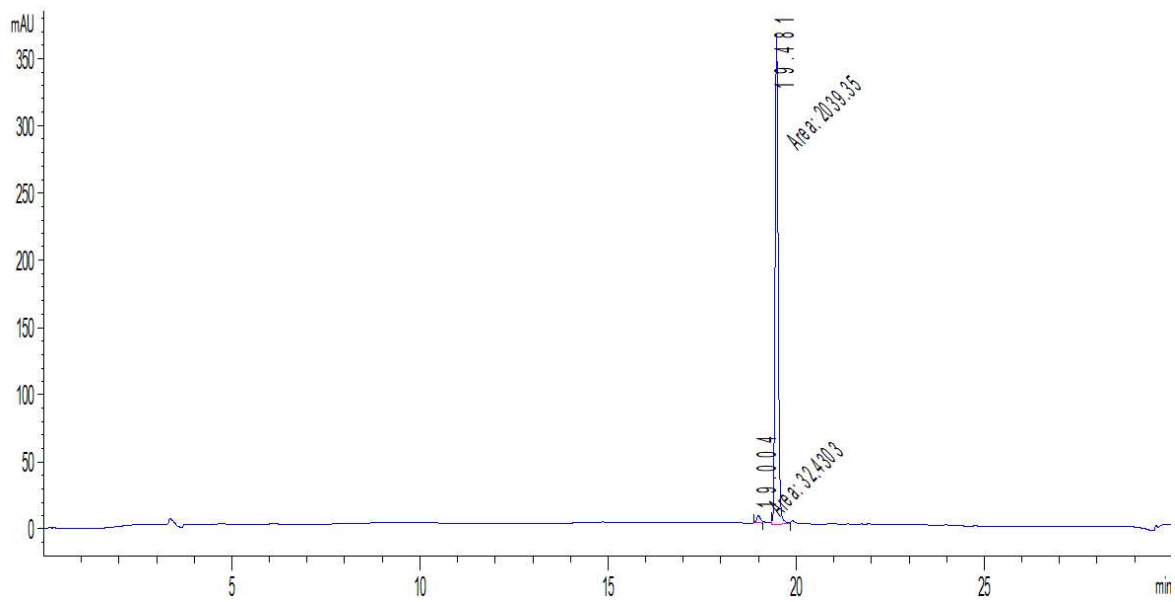
12a, HPLC system 2, $\lambda = 254$ nm



12b, HPLC system 2, $\lambda = 254$ nm



13, HPLC system 1, $\lambda = 254$ nm



Supplementary References.

1. Zhang, C.; Srinivasan, Y.; Arlow, D. H.; Fung, J. J.; Palmer, D.; Zheng, Y.; Green, H. F.; Pandey, A.; Dror, R. O.; Shaw, D. E.; Weis, W. I.; Coughlin, S. R.; Kobilka, B. K. High-Resolution Crystal Structure of Human Protease-Activated Receptor 1. *Nature* **2012**, *492*, 387-392.
2. Cheng, R. K. Y.; Fiez-Vandal, C.; Schlenker, O.; Edman, K.; Aggeler, B.; Brown, D. G.; Brown, G. A.; Cooke, R. M.; Dumelin, C. E.; Dore, A. S.; Geschwindner, S.; Grebner, C.; Hermansson, N. O.; Jazayeri, A.; Johansson, P.; Leong, L.; Prihandoko, R.; Rappas, M.; Soutter, H.; Snijder, A.; Sundstrom, L.; Tehan, B.; Thornton, P.; Troast, D.; Wiggin, G.; Zhukov, A.; Marshall, F. H.; Dekker, N. Structural Insight into Allosteric Modulation of Protease-Activated receptor 2. *Nature* **2017**, *545*, 112-115.
3. Kennedy, A. J.; Ballante, F.; Johansson, J. R.; Milligan, G.; Sundström, L.; Nordqvist, A.; Carlsson, J. Structural Characterization of Agonist Binding to Protease-Activated Receptor 2 Through Mutagenesis and Computational Modeling. *ACS Pharmacol. Transl. Sci.* **2018**, *1*, 119-133.
4. Maschauer, S.; Einsiedel, J.; Huebner, H.; Gmeiner, P.; Prante, O. 18F- and 68Ga-Labeled Neuropeptides for PET Imaging of Neuropeptides Receptor 1. *J. Med. Chem.* **2016**, *59*, 6480-6492.
5. McGuire, J. J.; Saifeddine, M.; Triggle, C. R.; Sun, K.; Hollenberg, M. D. 2-Furoyl-LIGRLO-Amide: A Potent and Selective Proteinase-Activated Receptor 2 Agonist. *J. Pharmacol. Exp. Ther.* **2004**, *309*, 1124-1131.
6. Yau, M. K.; Suen, J. Y.; Xu, W.; Lim, J.; Liu, L.; Adams, M. N.; He, Y.; Hooper, J. D.; Reid, R. C.; Fairlie, D. P. Potent Small Agonists of Protease Activated Receptor 2. *ACS Med. Chem. Lett.* **2016**, *7*, 105-110.
7. Behnam, M. A. M.; Nitsche, C.; Vechi, S. M.; Klein, C. D. C-Terminal Residue Optimization and Fragment Merging: Discovery of a Potent Peptide-Hybrid Inhibitor of Dengue Protease. *ACS Med. Chem. Lett.* **2014**, *5*, 1037-1042.
8. Ager, D. J.; Prakash, I. Reductions of Aromatic Amino Acids and Derivatives. *Org. Process Res. Dev.* **2003**, *7*, 164-167.
9. Zhang, S.; Govender, T.; Norstroem, T.; Arvidsson, P. I. An Improved Synthesis of Fmoc-N-Methyl- α -Amino Acids. *J. Org. Chem.* **2005**, *70*, 6918-6920.
10. Maennel, B.; Dengler, D.; Shonberg, J.; Huebner, H.; Moeller, D.; Gmeiner, P. Hydroxy-Substituted heteroarylpirazoles: Novel Scaffolds for β -Arrestin-Biased D2R Agonists. *J. Med. Chem.* **2017**, *60*, 4693-4713.
11. Strober, W. Trypan Blue Exclusion Test of Cell Viability. *Curr. Protoc. Immunol.* **1997**, *21*, A.3B.1-A.3B.2.
12. Baell, J. B.; Holloway, G. A. New Substructure Filters for Removal of Pan Assay Interference Compounds (PAINS) from Screening Libraries and for Their Exclusion in Bioassays. *J. Med. Chem.* **2010**, *53*, 2719-2740.

13. Sterling, T.; Irwin, J. J. ZINC 15 - Ligand Discovery for Everyone. *J. Chem. Inf. Model.* **2015**, *55*, 2324-2337.

14. Anandakrishnan, R.; Aguilar, B.; Onufriev, A. V. H++ 3.0: Automating pK Prediction and the Preparation of Biomolecular Structures for Atomistic Molecular Modeling and Simulations. *Nucleic. Acids. Res.* **2012**, *40*, W537-W541.

15. Lomize, M. A.; Lomize, A. L.; Pogozheva, I. D.; Mosberg, H. I. OPM: Orientations of Proteins in Membranes Database. *Bioinformatics* **2006**, *22*, 623-625.

16. Wolf, M. G.; Hoefling, M.; Aponte-Santamaria, C.; Grubmuller, H.; Groenhof, G. G_membed: Efficient Insertion of a Membrane Protein into an Equilibrated Lipid Bilayer with Minimal Perturbation. *J. Comput. Chem.* **2010**, *31*, 2169-2174.

17. Case, D. A.; Cerutti, D. S.; Cheatham, I., T. E. ; Darden, T. A.; Duke, R. E.; Giese, T. J.; Gohlke, H.; Goetz, A. W.; Greene, D.; Homeyer, N.; Izadi, S.; Kovalenko, A.; Lee, T. S.; LeGrand, S.; Li, P.; Lin, C.; Liu, J.; Luchko, T.; Luo, R.; Mermelstein, D.; Merz, K. M.; Monard, G.; Nguyen, H.; Omelyan, I.; Onufriev, A.; Pan, F.; Qi, R.; Roe, D. R.; Roitberg, A.; Sagui, C.; Simmerling, C. L.; Botello-Smith, W. M.; Swails, J.; Walker, R. C.; Wang, J.; Wolf, R. M.; Wu, X.; Xiao, L.; York, D. M.; Kollman, P. A. AMBER17. *University of California, San Francisco* **2017**.

18. Wang, J.; Wolf, R. M.; Caldwell, J. W.; Kollman, P. A.; Case, D. A. Development and Testing of a General Amber Force Field. *J. Comput. Chem.* **2004**, *25*, 1157-1174.

19. Maier, J. A.; Martinez, C.; Kasavajhala, K.; Wickstrom, L.; Hauser, K. E.; Simmerling, C. ff14SB: Improving the Accuracy of Protein Side Chain and Backbone Parameters from ff99SB. *J. Chem. Theory. Comput.* **2015**, *11*, 3696-3713.

20. Bayly, C. I.; Cieplak, P.; Cornell, W.; Kollman, P. A. A Well-Behaved Electrostatic Potential Based Method Using Charge Restraints for Deriving Atomic Charges: the RESP Model. *J. Phys. Chem.* **1993**, *97*, 10269-10280.

21. Van Der Spoel, D.; Lindahl, E.; Hess, B.; Groenhof, G.; Mark, A. E.; Berendsen, H. J. GROMACS: Fast, Flexible, and Free. *J. Comput. Chem.* **2005**, *26*, 1701-1718.

22. Abraham, M. J.; Murtola, T.; Schulz, R.; Páll, S.; Smith, J. C.; Hess, B.; Lindahl, E. GROMACS: High Performance Molecular Simulations Through Multi-Level Parallelism from Laptops to Supercomputers. *SoftwareX* **2015**, *1-2*, 19-25.

23. Darden, T.; York, D.; Pedersen, L. Particle Mesh Ewald - an N.Log(N) Method for Ewald Sums in Large Systems. *J Chem Phys* **1993**, *98*, 10089-10092.

24. Saleh, N.; Ibrahim, P.; Saladino, G.; Gervasio, F. L.; Clark, T. An Efficient Metadynamics-Based Protocol to Model the Binding Affinity and the Transition State Ensemble of G-Protein-Coupled Receptor Ligands. *J. Chem. Inf. Model.* **2017**, *57*, 1210-1217.

25. Laio, A.; Parrinello, M. Escaping Free-Energy Minima. *Proc. Natl. Acad. Sci. U.S.A.* **2002**, *99*, 12562-12566.

26. Barducci, A.; Bussi, G.; Parrinello, M. Well-Tempered Metadynamics: a Smoothly Converging and Tunable Free-Energy Method. *Phys. Rev. Lett.* **2008**, *100*, 020603.

27. Tribello, G. A.; Bonomi, M.; Branduardi, D.; Camilloni, C.; Bussi, G. PLUMED 2: New Feathers for an Old Bird. *Comput. Phys. Commun.* **2014**, *185*, 604-613.

28. Hanwell, M. D.; Curtis, D. E.; Lonie, D. C.; Vandermeersch, T.; Zurek, E.; Hutchison, G. R. Avogadro: an Advanced Semantic Chemical Editor, Visualization, and Analysis Platform. *J. Cheminform.* **2012**, *4*, 17.

29. Trott, O.; Olson, A. J. AutoDock Vina: Improving the Speed and Accuracy of Docking with a New Scoring Function, Efficient Optimization, and Multithreading. *J. Comput. Chem.* **2010**, *31*, 455-461.

30. Case, D. A.; Ben-Shalom, I. Y.; Brozell, S. R.; Cerutti, D. S.; Cheatham, T. E.; III; Cruzeiro, V. W. D.; Darden, T. A.; Duke, R. E.; Ghoreishi, D.; Gilson, M. K.; Gohlke, H.; Goetz, A. W.; Greene, D.; Harris, R.; Homeyer, N.; Izadi, S.; Kovalenko, A.; Kurtzman, T.; Lee, T. S.; LeGrand, S.; P. Li, C. L.; Liu, J.; Luchko, T.; Luo, R.; Mermelstein, D. J.; Merz, K. M.; Miao, Y.; Monard, G.; Nguyen, C.; Nguyen, H.; Omelyan, I.; Onufriev, A.; Pan, F.; Qi, R.; Roe, D. R.; Roitberg, A.; Sagui, C.; Schott-Verdugo, S.; Shen, J.; Simmerling, C. L.; Smith, J.; Salomon-Ferrer, R.; Swails, J.; Walker, R. C.; Wang, J.; Wei, H.; Wolf, R. M.; Wu, X.; Xiao, L.; York, D. M.; Kollman, P. A. AMBER 2018. *University of California, San Francisco* **2018**.

31. Frisch, M. J.; Trucks, G. W.; Schlegel, H. B.; Scuseria, G. E.; Robb, M. A.; Cheeseman, J. R.; Scalmani, G.; Barone, V.; Petersson, G. A.; Nakatsuji, H.; Li, X.; Caricato, M.; Marenich, A. V.; Bloino, J.; Janesko, B. G.; Gomperts, R.; Mennucci, B.; Hratchian, H. P.; Ortiz, J. V.; Izmaylov, A. F.; Sonnenberg, J. L.; Williams-Young, D.; Ding, F.; Lipparini, F.; Egidi, F.; Goings, J.; Peng, B.; Petrone, A.; Henderson, T.; Ranasinghe, D.; Zakrzewski, V. G.; Gao, J.; Rega, N.; Zheng, G.; Liang, W.; Hada, M.; Ehara, M.; Toyota, K.; Fukuda, R.; Hasegawa, J.; Ishida, M.; Nakajima, T.; Honda, Y.; Kitao, O.; Nakai, H.; Vreven, T.; Throssell, K.; Montgomery, J. A., Jr.; Peralta, J. E.; Ogliaro, F.; Bearpark, M. J.; Heyd, J. J.; Brothers, E. N.; Kudin, K. N.; Staroverov, V. N.; Keith, T. A.; Kobayashi, R.; Normand, J.; Raghavachari, K.; Rendell, A. P.; Burant, J. C.; Iyengar, S. S.; Tomasi, J.; Cossi, M.; Millam, J. M.; Klene, M.; Adamo, C.; Cammi, R.; Ochterski, J. W.; Martin, R. L.; Morokuma, K.; Farkas, O.; Foresman, J. B.; Fox, D. J. Gaussian 16. **2016**.